Microalgal Production of Biodiesel and Lutein

A Technical Report submitted to the Department of Chemical Engineering

Presented to the Faculty of the School of Engineering and Applied Science

University of Virginia • Charlottesville, Virginia

In Partial Fulfillment of the Requirements for the Degree of

Bachelor of Science in Chemical Engineering

School of Engineering and Applied Science

Spring 2024

Technical Project Team Members:

Soren Andrews

Cynthia Bing-Wo

Alex Hawkins

Aydan Moskowitz

Pablo Newton

On my honor as a University Student, I have neither given nor received unauthorized aid on this assignment as defined by the Honor Guidelines for Thesis-Related Assignments

Eric Anderson, Department of Chemical Engineering

Table of Contents

List of Figures

List of Tables

Executive Summary

The following report details the design of an algae farm and biofuel refinery plant. The recommended design presented in this report is built upon Aspen Plus modeling, research literature, and chemical engineering principles. Motivation for pursuing this plant design stems from the current need for alternative fuel sources in response to global climate change action. An economic analysis on the recommended design will be used to determine its viability and feasibility of implementation. An analysis of safety and environment will be presented to determine the desirability of the recommended design.

The process described in this paper begins with algae cultivation and harvesting. The algae species, *Chlorella vulgaris*, is grown in open raceway ponds containing a nutrient media formed from swine waste. During harvesting, algae is concentrated via dissolved air floatation. To remove valuable lipids inside the algae, a cell disruption process will be used to release algae components followed by a lipid extraction using solvent washing. Lipids are then reacted using acid esterification and base transesterification to form the fatty acid methyl esters (FAME) that constitute biodiesel. During the esterification reactions, lutein will be co-produced as the plant's secondary product. Separation of FAME and lutein will occur via two liquid-liquid extractions with various solvents. A final distillation will be used to refine the FAME to its objective purity while anti-solvent precipitation will be used to generate pure lutein crystals.

The plant will operate on a 11-month schedule where algae growth rates are dependent on seasonal local weather. In a year of production, the plant generates an estimated 20.5 million gallons of FAME and 547,000 kg of Lutein. With assumed market prices of $4.6/gal FAME and $60/kg Lutein, the resulting yearly product revenue is $128 million. The recommended design requires a yearly operating cost of $407 million. Subsequently, plant operation results in a loss of

$279 million per year. Given the economic results, the recommended design is not a viable option for biofuel production from algae.

1. Introduction

1.1 Background

As the impacts of climate change become increasingly apparent, efforts to mitigate global carbon emissions have intensified. In the United States, the largest contributor to greenhouse gas emissions in the economic sector comes from transportation, primarily from gasoline and diesel engines (EPA, 2023). Efforts to reduce transportation emissions using alternative fuels has led to the development of biodiesel as a substitute for petrol diesel used by heavy duty vehicles.

Biodiesel is produced through transesterification of lipids found in natural sources such as animal fats, vegetable oils, and algae (Guo, Song, & Buchain, 2015). Among these biodiesel sources, microalgae demonstrate high potential for commercial biodiesel production due to their high lipid content. The idea of using microalgae for fuel production was first introduced by Harder and von Witsch in 1942 (Borowitzka, 2013). In the following decades, research efforts led to the development of functional cultivation methods such as raceway ponds and closed reactors, enabling commercial production of algae. In 1980, The U.S. Department of Energy started the Algae Species Program (ASP) to explore algae as a source of biofuels, identifying species of high lipid content microalgae suitable for large scale cultivation. (Borowitzka, 2013).

While the ASP addressed scale-up issues surrounding cultivation, challenges still persist today in achieving high enough yields of biomass and lipids to make biodiesel production economically viable. Advances in lipid extraction and separation processes are essential to overcoming these economic barriers. Simultaneously, the production of value added products, such as carotenoids found in algae, can improve economic viability. *Chlorella vulgaris* is a strain of microalgae that contains sufficient lipid content and the carotenoid lutein. Lutein is an important nutrient for eye health as it has demonstrated potential for reducing the onset of ocular

diseases such as age related macular degeneration and cataracts (Alves-Rodrigues & Shao, 2004). Lutein is typically consumed through dark leafy greens such as spinach and kale, however, changes in the diet of Americans have resulted in lower lutein consumption. This shift in consumption, coupled with the recognized health benefits of lutein, has created a market for lutein-based nutraceuticals. This emerging market for lutein, along with breakthroughs in algal lipid separation techniques, could aid in facilitating commercialization of algae based biodiesel.

1.2 Product Information

The primary product of interest is fatty acid methyl ester (FAME) biodiesel shown in Figure 1.2-01a. FAME biodiesel will be formulated as a 100% biodiesel blend stock otherwise known as B100. The biodiesel stock will be sold to manufacturers to be turned into B20 and B6 diesel blends to be used in diesel engines. B100 produced by the plant must meet quality specifications under an international standard called ASTM D6751. Under this standard, B100 must not exceed 0.2 wt% methanol, 0.05% volume water, 0.5 mg KOH/g, and 0.24 wt% glycerin (AFDC, 2023). ASTM D6751 also outlines fluid property requirements such as flash point and viscosity.

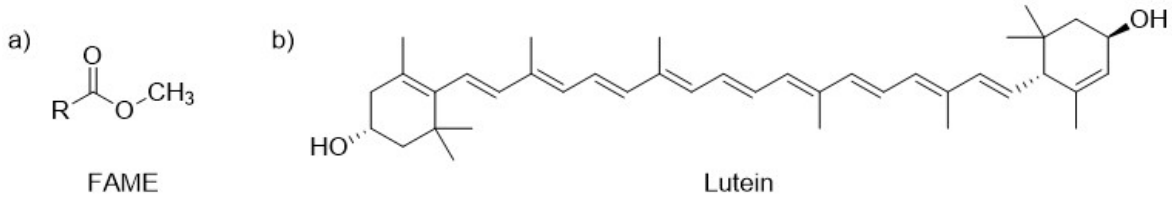

Figure 1.2-01: a) Chemical structure of fatty acid methyl ester biodiesel; b) Chemical structure of free lutein.

The secondary product is lutein shown in Figure 1.2-01b. Lutein will be formulated as a crystalline solid and sold to manufacturers as a stock for lutein based nutraceuticals. Examples of

products include eye vitamins originating from the AREDS2 study and general lutein supplements. Lutein product will contain amounts of its stereoisomer zeaxanthin. A lutein reference chromatogram published by the USP showed that the ratio of lutein to zeaxanthin was 12.6:1 corresponding to a lutein purity of 96%. This purity will serve as the basis for the plant's final lutein product.

1.3 Starting Materials

The algae species used in this process is *Chlorella vulgaris.* This particular species was chosen due to its relatively high lipid content and its ability to produce lutein ester. Particular strains of *C. vulgaris* have demonstrated growth in heterotrophic conditions, providing an advantage over light dependent strains during cultivation.

Algae will be grown in open raceway ponds containing a nutrient rich media made from water and local piggery (swine) waste. Swine waste will provide the nitrogen, carbon, and phosphorus needed to promote algae growth. It will be readily available at a low price due to the large number of pig farms in the region surrounding the plant. Municipal utility water will dilute the swine waste to form the final nutrient media. Water will be recycled after algae harvesting to minimize costs and strain on the municipal water supply.

Free fatty acids, triglycerides, and lutein ester will be extracted and separated using chloroform, methanol, and water as solvents. Methanol will also be used in the esterification reactions that produce the final FAME and lutein products. Sulfuric acid (H_2SO_4) and potassium hydroxide (KOH) will serve as acid/base catalysts in these reactions. Hexane and ethanol will be used to separate the final FAME and lutein products via extraction. Choices of extraction solvents in the overall process are inspired by work from Prommuak et al. (2012).

1.4 Scale

Based on the final recommended design, the production rate of FAME and lutein is estimated to be 225.6 ton/day and 1.823 ton/day respectively. The yearly production rate based on the proposed production schedule is 20,520,000 gal/yr of FAME and 552,300 kg/yr of lutein.

1.5 Location

The plant will be located in Duplin County, North Carolina due to the availability of pig waste as a low cost in the area. Smithfield Hog Production, located in Warsaw within Duplin County, is a massive livestock production facility (Smithfield Foods, n.d.). Additionally, there are other hog production farms throughout the county. These are all used to support the large swine waste requirement for the algae cultivation with the location choice eliminating supply issues for the nutrient sourcing.

2. Previous Work

A technical report presented by Black et al. (2022) to the University of Virginia Department of Chemical Engineering in the spring 2022 detailed a design for an algae farm and biodiesel refinery plant for the coproduction of FAME and glycerol from *C. vulgaris*.

Their recommended plant design produced an estimated 4,528,000 gal/yr of FAME and 203,200 gal/yr of glycerol. After examination of plant economics, Black et al. (2022) did not recommend the continuation of the plant's design. With the 2022 market prices of FAME and glycerol, plant operation would result in a loss of $15.9M/yr. Black et al. (2022) provided recommendations for possibly improving the economic viability of their plant design. Such recommendations included eliminating glycerol refinement steps, increased biodiesel prices, and free agricultural waste as a nutrient source.

The plant design described in the following sections aims to improve upon the work by Black et al. (2022). Rather than refining glycerol, this plant design aims to co-produce lutein, which has a higher market value with projected strong growth potential over the course of the plant's lifetime. The plant design will also make use of separation techniques to recover and reuse a majority of solvents required for extraction and reaction operations. Lastly, algae cultivation will make use of unwanted excess swine waste from local pig farms at a negligible cost.

3. Discussion

The entire process is broken down into four sections: algae cultivation, crude lipid extraction, lipid esterification, and product formation. In the first section, the algae feedstock is grown, harvested, and dried into the biomass feed for downstream operations. The second section entails removing key components from the biomass via solvent extraction. These extracted components comprise free fatty acids, triglycerides, and free lutein that is reacted in the third section to form FAME and lutein. Finally, the fourth section separates and purifies the FAME and Lutein products to the desired specifications. Figure 3.0-01 illustrates this process overview in a block flow diagram. A more detailed process flow diagram for each section that includes stream and equipment tag numbers will be presented in the Recommended Design section of this report.

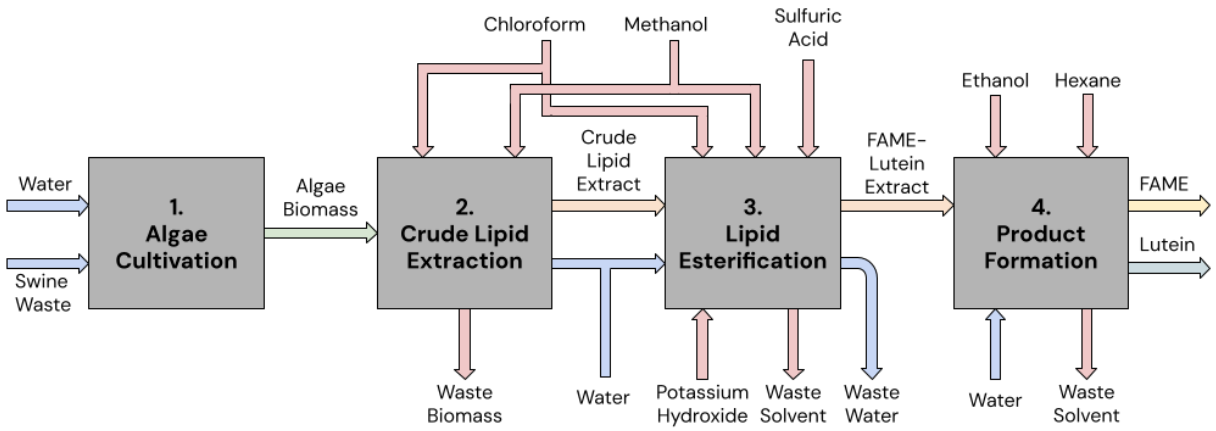

Figure 3.0-01: Process overview block diagram

3.1 Algae Cultivation

Algae can be grown using a variety of methods, the most common being raceway cultivation and photobioreactors. Open air raceways are less expensive than photobioreactors in

terms of both operating and capital costs but are more prone to contamination from other algae (Narala et al., 2016). Photobioreactors offer a more controlled environment with complete light exposure and tend to support higher cell densities (Banerjee & Ramaswamy, 2019). Because *C. vulgaris* is heterotrophic, light is not required for growth, and the algae is able to survive on the nutrients it eats. This, coupled with the fact that photobioreactors are hard to scale up, makes them an unnecessary expense. A comprehensive process flow diagram covering discussion sections 3.1-3.4 can be found in recommended design section 4.1.

3.1.1 Raceway Design (R-101)

The raceway structure was determined using insights from Kumar et al. (2015). Figure 3.1-01 shows the raceway geometry and dimensions. To minimize energy loss of the fluid's momentum, an ovular design with two long straights and two semi-circle curves was chosen. The dimensions were selected to be 5.8 meters wide by 35.4 meters long and 2.2 meters deep with a working depth of 2.0 meters. The length and width are preserved from the previous design by Black et al. (2022); however, the depth was increased due to heterotrophic growth conditions.

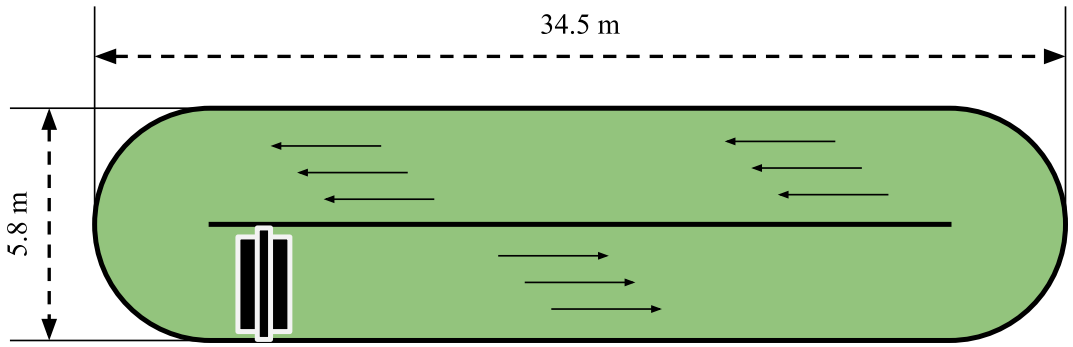

Figure 3.1-01: Raceway pond schematic

Raceway ponds will be constructed using packed gravel and a PVC liner that prevents leaking, similar to the conditions described in Black et al. (2022). To prevent settling, the algae

must be cultivated in turbulent fluid conditions maintained by a paddle wheel system. To ensure a minimum average required fluid velocity of 0.1 m/s throughout the raceway, the paddle wheel should produce a fluid velocity of 0.2 m/s (Chisti, 2013). The paddles will operate at a rotational velocity of 20 rpm to maintain the fluid velocities described above (Pandley & Premalatha, 2017). The paddles will be configured with their axis of rotation slightly above the water level; to ensure roughly ten centimeters of clearance from the bottom of the raceway, the paddle wheel diameter will be 4.27 m or 14 ft. To ensure that fluid conditions are turbulent, the Reynolds Number can be calculated using (3-01) where ρ_l is the density of the fluid, D_h is the wetted perimeter of the raceway. The density and viscosity of the fluid was taken as a weighted average where the density of fresh pig manure is 760 kg/m^3 and water is 1000 kg/m^3, and the viscosity of pig manure is 3.65cP and water is 1cP (Andersen, 2018; Yu, 2018). The temperature of the fluid was assumed to be 70^{o}F, the average year-round water temperature in Duplin County, NC. Using the conditions described, a Reynolds number of $5.7 \cdot 10^5$ can be achieved which confirms turbulent flow. To calculate the power required to support the paddles, a raceway power equation (3-02) provided by Christi (2013) can be used, where L_r is the total length of the raceway, g is gravity, u is linear velocity, f_M is the Manning roughness factor, and e is the motor, drive, and paddle wheel efficiency. Due to the materials of construction, the Manning roughness factor can be approximated as 0.012. For a flat-bottomed raceway channel, the efficiency is 0.17 (Chisti, 2013). To support a paddle wheel-generated fluid velocity of 0.2m/s, the power required is approximately 47 Watts. Motors that match this output can be used, but as motors are generally not very expensive and there is risk of dead spots in the tank necessitating a higher RPM, a higher powered motor is also a viable option.

$$R = \frac{\rho_l D_h U_l}{\mu_l} \tag{3-01}$$

$$P = \frac{1.59 \rho g u^3 L_r f_M^2 (w+2h)}{e D_h^{0.33}} \tag{3-02}$$

3.1.2 Algae Growth

To support the growth of *C. vulgaris,* the nutrient source for the algae was chosen to be swine waste. The plant site is located in Duplin County, NC, where swine waste is readily available at low cost; a tank will be onsite for trucks to offload into that was designed to hold a slightly larger volume than one raceway. The additional tank step and subsequent pumping with make-up water should break up the majority of solids in the waste, creating a mixture with less variances in density and avoiding dumping waste directly into the raceways. The swine waste contains the nitrogen, phosphorus, and sulfur required for algae cultivation. Nitrogen will be the limiting nutrient at a concentration of 51.3 lb Nitrogen/1,000 gallons waste (Chastain et al., n.d.). Using growth data from Sakarika et al. (2017), Nitrogen limiting conditions suggest a cell density of 11.19 g/L will be obtained after a twenty day growth period. Taking into account yield losses with scale-up, a cell density during harvest of 10 g/L was determined to be appropriate.

3.1.3 Growth Schedule

Assuming a peak production of 25,000,000 kg of algae in one month, the total number of raceways required was calculated to be 4,321. This was based on a batch schedule with one batch of 216 raceways producing 833,000 kg of algae finishing each day. After a batch finished, the correlating raceways would be drained and refilled with recycled water and additional waste slurry, using the algae in the recycled water as a seed for the next batch. From this model, there would be approximately 78M kg of water and 5.2M kg of swine waste required to fill one batch.

Outside of peak production months, the batch schedule remains the same, with seasonal temperatures being taken into account to determine how much the growth rate will diminish. The growth efficiencies were estimated based on the optimum temperature of 25℃ for the growth of *C. vulgaris* (Josephine et al., 2022). In addition, the average monthly temperatures in Kenansville, NC according to WeatherSpark.com were used to estimate growth efficiency based on their deviation from 25℃ (“Kenansville Climate”, n.d.). Table 3-01 shows the monthly production estimates based on changing growth efficiency due to seasonal temperature changes.

Table 3.1-01
Monthly Algae Biomass Yield

Month	**Growth Efficiency (%)**	**Algae Produced (kg)**	**Days in Month**
January	0.25	1,562,500	31
February	0.25	1,562,500	28
March	0.25	1,562,500	31
April	0.75	14,062,500	30
May	0.85	18,062,500	31
June	1.00	25,000,000	30
July	1.00	25,000,000	31
August	1.00	25,000,000	31
September	0.85	18,062,500	30
October	0.75	14,062,500	31
November	0.25	1,562,500	30
December	0	0	31
Total		145,500,000	

3.2 Biomass Dewatering

Following cultivation in the raceways, the algae exists as a dilute suspension in water composed of 1% algae by weight (Sakarika et al., 2017). As a result, the algae must be harvested in order to concentrate and dewater it to promote effective lipid extraction (Danquah et al., 2009). There are several techniques for dewatering, including filtration, flocculation, flotation, centrifugation, and sedimentation (Sukenik et al., 1988). In this instance, flotation was chosen as an initial dewatering step due to the relatively low cost of operation and the lack of chemical flocculants. In addition, the collected algal slurry from flotation is ideal for wet bead milling (due to the remaining water content), which was chosen as the method to lyse the algae cells. Further dewatering is still needed after lysis and will be discussed further in section 3.4.

3.2.1 Dissolved Air Flotation (V-101,102)

Flotation has proven successful at large scales, offering a cost-effective method for harvesting algae with a moderate energy requirement (Leite et al., 2019). One type specifically: dissolved air flotation (DAF), introduces a stream of fine bubbles between 10 and 100 μm in diameter of air into the water that attach to the algae particles, causing them to float to the surface, forming a scum layer that can be removed (Niaghi et al., 2015). To enhance the recovery process, DAF is often combined with the addition of coagulants and flocculants. However, this approach requires a continuous chemical input, can risk potential contamination, and necessitates additional purification steps, contributing to high cost. As a result, chemical flocculants will not be used in this project. A study conducted by Niaghi et al. (2015) optimized operating conditions for a DAF unit without the use of chemical flocculants, achieving 91% algae recovery. This process additionally reduced costs through low air-saturated water consumption and minimal

energy requirements through low operating pressure. Their results recommend an inlet algae concentration exceeding 500 mg algae/L. The algae solution entering DAF contains 10 g algae/L, verifying the applicability of this study.

The DAF unit consists of a saturator and a flotation tank. Compressed air will be fed to the saturator at a pressure of 3 atm as described by Niaghi et al. (2015) for the optimum saturator operating conditions. The total amount of air required for saturation was determined from the solubility of air at 3 atm in 70 °F water according to The Engineering Toolbox. This value was reported as 0.072 volume of air/volume of water. 70 °F water temperature was chosen because it is the average water temperature in Duplin County throughout the year, and the variation of the ambient water temperature throughout the year is minimal and would have very little effect on the solubility of air. It was also assumed that the raised temperature of the pressurized air would have little effect on the temperature of the water and thus the solubility of the air since the mass of the air is negligible compared to the mass of the water. In the saturator, water is infused with air, creating a solution that is then directed to the flotation tank. In the flotation tank, a sudden pressure reduction generates microbubbles within the water. It is designed with two inlets: one for air-saturated water from the saturator and another for the introduction of the algae solution. The algae adheres to the microbubbles and are carried to the surface. Algae sludge will be hydraulically removed over a weir as the water level in the tank rises. One portion of the remaining water will be reused and reintroduced into the saturator. The rest will be recycled back into the raceways to decrease water requirements and act as an inoculant. A representative schematic of the dissolved air flotation system is shown in Figure 3.2-01 as depicted by Fuad et al. (2021). Note, the regions numbered 1-3 are all a part of the flotation tank while region 4 is a separate hopper attached to the system to collect the algae.

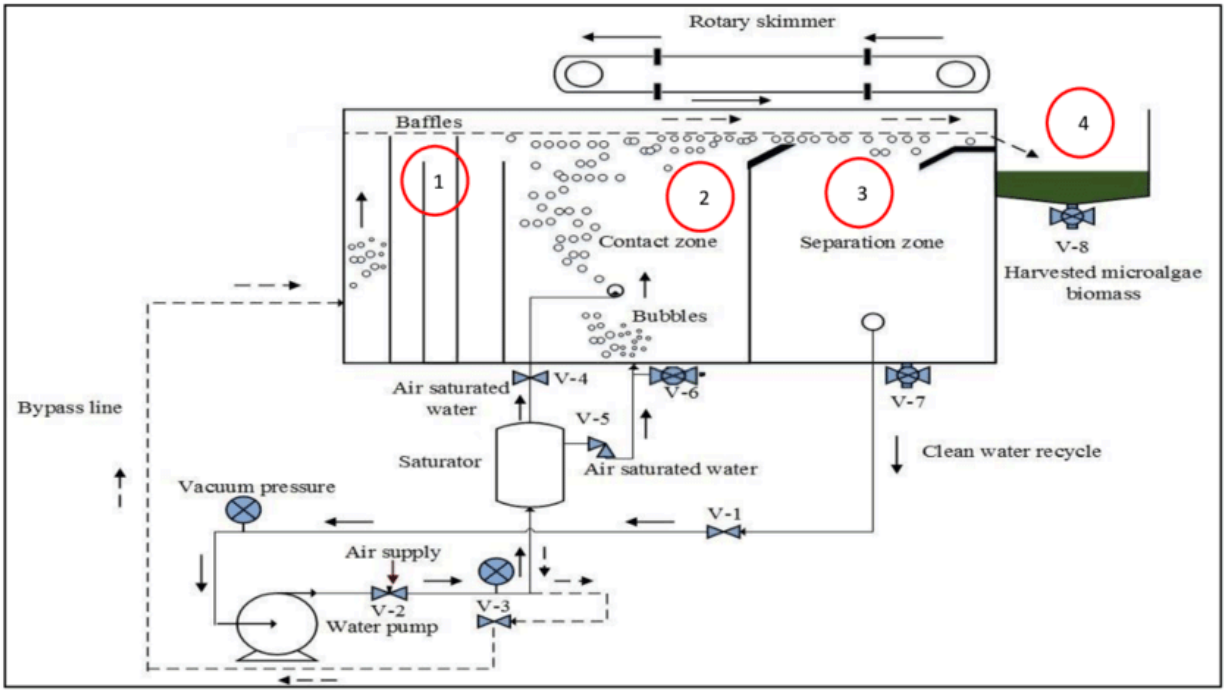

Figure 3.2-01: Dissolved air flotation schematic (Fuad et al., 2021)

The study by Niaghi et al. (2015) lacks information on the composition of the outlet algae solution. As a result, drawing on data from Uduman et al. (2010), it is assumed that the algae concentration leaving the DAF will be 6% by dry algal weight.

3.2.2 Nanomagnetite Flocculants

Nanomagnetite particles have gained recent recognition for their potential as a method for harvesting algal biomass, emerging as an alternative to flotation and chemical flocculation. Magnetic separation is cost-effective, conventional, easy to operate, environmentally friendly, and achieves high yields (Patel et al., 2022). These particles adsorb to algae cells through interactions such as hydrogen bonds, electrostatic, Van der Waals, hydrophobic, and hydrophilic forces (Taghizadeh et al., 2020). After use, the nanomagnetite particles may be recovered and reused, substantially minimizing costs. Patel et al. (2022) and Savvidou et al. (2021) have developed iron-based nanoparticles that exhibit a harvesting efficiency of 99% after one use and

continue to be above 85% efficient after five cycles without diminishing the quality of the biomass. Savvidou et al. (2021) determined the adsorption capacity to be 22.95 g biomass/g nanomagnetite particle. This design is considered due to high harvesting efficiency, though high cost of large quantities of nanomagnetite particles may prevent implementation. Nanomagnetite flocculation may be combined with DAF to increase biomass recovery while reducing the amount of nanomagnetite particles needed, however literature values for this approach do not exist at this time.

3.3 Bead Milling (R-102)

Following the dewatering process, the algae will undergo a disintegration procedure to damage and break the cell wall to enable sufficient extraction of various types of lipid molecules, including free fatty acids (FFAs), triglycerides, and lutein esters during the lipid extraction process. Cell disintegration will be performed using a technique called bead milling where cells are damaged through kinetic collisions from high velocity beads. Recent advancements in bead mill design, temperature control, and the ability to operate continuously have made bead milling a suitable disintegration technique for *C. vulgaris* compared to enzymatic, chemical, and ultrasonication methods (Postma et al., 2015). Within the bead mill, the rate at which cells are disintegrated follows first order kinetics as shown by (3-03), where n_{exit} is the concentration of intact cells leaving the bead mill and k_{dis} is the kinetic cell disintegration constant (Suarez-Garcia et al., 2019).

$$r = k_{dis} \cdot n_{exit} \tag{3-03}$$

The efficiency of cell wall disintegration in a bead mill is dependent on a multitude of parameters, particularly bead diameter, bead filling ratio, and suspension flow rate (Postma et al.,

2017). The selection of bead size, bead material, and bead fill fraction was determined using an optimization study from Postma et al. (2017). Results from the study determined that a bead diameter of 0.40mm yielded the highest cell disintegration rates for *C. vulgaris*, producing a maximum reported k_{dis} value of 0.041 ± 0.003 s^{-1}. The bead milling procedure from Postma et al. (2017) used Yttrium stabilized ZrO2 beads at a filling volume of 65% v/v. Therefore, the final bead mill design will incorporate 0.40 mm diameter Tosoh YTZ beads with a fill volume of 65% v/v in effort to maintain the same milling conditions as used in Postma et al. (2017).

A set of equations modeling a bead mill operated in batch recirculation mode was used to support scale and flow rate calculations (Suarez-Garcia et al., 2019). Equations and relevant nomenclature are presented in Figure 3.3-01. The set of equations were solved to determine the suspension flow rate (F) and feed tank volume (V_f) for a given mill chamber volume (V_{ch}) , such that k_{dis} would match the value presented by Postma et al. (2017).

Bead Mill Design Equations

Kinetics Constant	$k_{dis} = \frac{F}{V_f}\left(1 - \frac{F}{F + k_D V_{ch}}\right)$
Cell Death Constant	$k_D = \frac{V_x}{V_{ch}} \eta \frac{E}{E_x}$
Energy from Colliding Beads	$E = \sum_{j=1}^{jm} E_{bj} \cdot z_j \cdot V_j$
Kinetic Energy of Beads	$E_b = \rho_b V_b u_b^2$
Frequency of Collisions	$z = \frac{\sqrt{2}}{2} u_b \pi d_b^2 n^2$
Velocity Profile	$u_b = u_L\left(1 - exp\left(-\frac{18\mu}{\rho_b d_b^2} t\right)\right)$
Bead Velocity	$u_L = \frac{\Omega \kappa^2}{1-\kappa^2}\left(\frac{R^2}{r} - r\right)$

Nomenclature

V_{ch} = *Mill chamber volume*
V_f = *Feed tank volume*
F = *Suspension flow rate*
Ω = *Agatator angular velocity*
R = *Mill chamber radius*
κ = *Ratio of agitator to chamber radius*
d_b = *Bead diameter*
ρ_b = *Bead specific density*
η = *Bead number density*
V_x = *Specific cell volume*
E_x = *Specific cell disintegration energy*
μ = *Suspension viscosity*

Figure 3.3-01: Bead mill design equations and nomenclature (Suarez-Garcia et al., 2019)

The following assumptions were made to the set of equations in Figure 3.3-01. First, it is assumed that the beads instantaneously reach their maximum velocity such that $u_b=u_L$ at all times. Secondly, beads are traveling at the same velocity as the outermost part of the agitator such that $r=\kappa R$ at all times. After applying these simplifying assumptions, the equations in Figure 3.3-01 were solved in MATLAB R2020a to determine the milling conditions needed to obtain a k_{dis} of 0.041 s^{-1}. Then, the resulting milling flow rate (F) and DAF feed flow rate (B) were calculated from material balance equations such that a steady state fraction of disrupted algae of 0.78 would leave the mill. Figure 3.3-02 shows the schematic for a single bead mill set-up in continuous recycle mode and resulting fraction disintegration profile from startup to steady state.

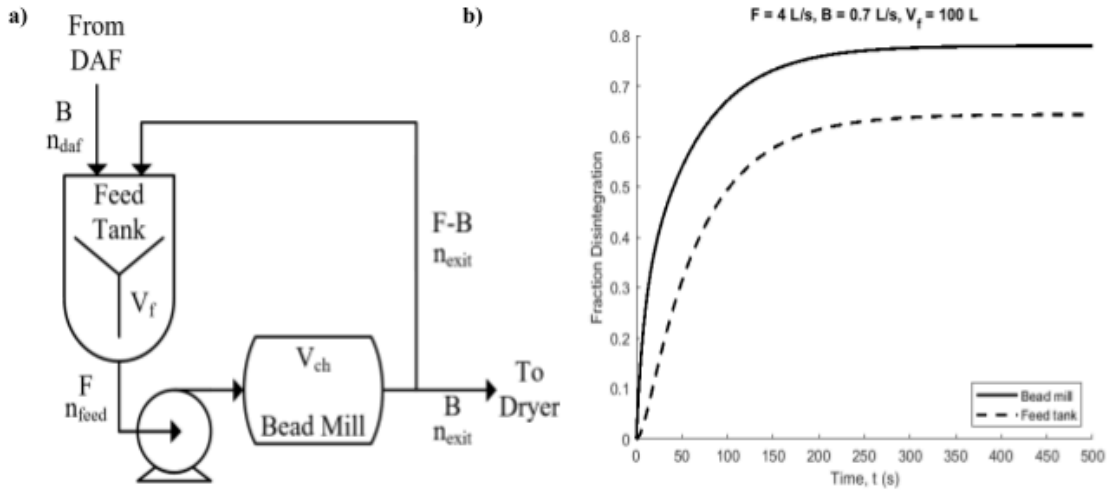

Figure 3.3-02: a) Bead milling schematic; b) Plot of fraction algae disintegration inside the feed tank and bead mill.

3.4 Biomass Drying (H-101)

The algae biomass must be dried to facilitate efficient downstream processing for effective lipid and lutein extraction. The drying operations are highly energy and cost intensive–it has been reported that drying can account for almost 60% of the energy required to

produce microalgal biofuels (Villagracia et al., 2016). The drying method therefore must be chosen appropriately to minimize costs while achieving a solution containing a target concentration of 90% algae (by weight). Common approaches include solar drying, convective drying, spray drying, cross-flow air drying, and freeze drying.

Solar drying is an environmentally-friendly and economical method of drying due to low energy costs but is slow and dependent on the weather. Convective drying is practical, but can lead to the degradation of biomass. Spray drying can achieve high efficiency at rapid drying times but incurs high energy requirements. Freeze drying simultaneously dries and lyses the algae, but exhibits extremely high costs for large scale operations. This project will utilize cross-flow air drying as a means to reach the desired moisture content while minimizing thermal damage to the algae. Cross-flow air drying employs a stream of hot air in order to dry the biomass. It is relatively fast compared to other dewatering techniques, but it also has a high energy cost (Kim, 2022). In addition to preventing thermal damage to the algae, cross-flow air drying can dry the biomass to similar levels as lyophilization without the loss of the desired organic materials contained within the cells. Other mechanical forms of dewatering, such as pressing or squeezing the biomass would result in loss of the desired lipid molecules because at this point the cells are already lysed and both water and lipids alike would be pressed out of the biomass. Therefore, the cross-flow drying will be achieved by evenly distributing the wet, lysed algae onto a continuously moving conveyor belt as a countercurrent stream of air flows over it. Conveyor belt dryers offer the benefit of the ability to operate at a low temperature. This decreases fire risks, the amount of volatile organic compounds produced, the energy consumption, and potential cell damage (Hosseinizand et al., 2017). The design for the dryer is modeled after that proposed by Hosseinizand et al., who studied optimal dryer conditions to

attain a final moisture content of 10%. Bed length and residence time were extrapolated from data values provided by Hosseinizand et al.

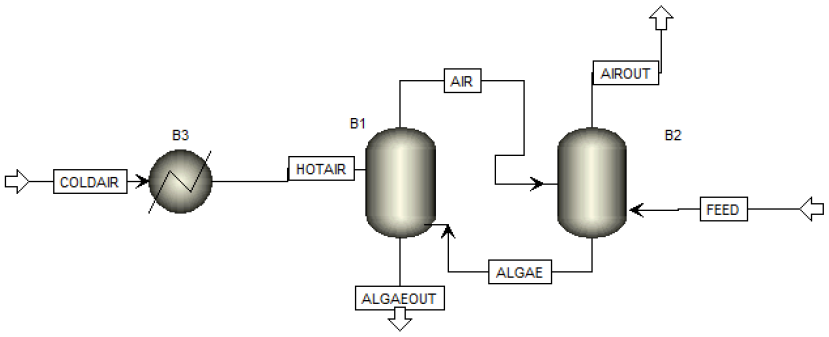

Figure 3.4-01. Cross flow dryer model Aspen flowsheet.

The conveyor belt dryer was modeled in Aspen, shown in Figure 3.4-01. Two Flash2 blocks were used to simulate cross-flow drying wherein a temperature gradient was created over blocks B1 and B2, which were set to operating temperatures of 80°C and 60°C respectively. NRTL was used as a base method, and nitrogen and oxygen were considered Henry components. The total water content of the inlet stream was calculated using a material balance around the bead mills after taking into account the water content of the lysed cells and the cell lysing efficiency. The cells and cell lysate were not included as solid components in the model and only the water and general lipids content based on weight percentages were taken into account for material flows. Then, a 10% desired water content in the effluent was chosen to preserve the same drying conditions used by Hosseinizand et al. (2017). These conveyor belt dryer specifications include the following parameters: 39 m bed length, 3.0 m bed width, 5.0 cm material depth on conveyor belt, air velocity of 1.0 m/s, ambient air pressure, inlet drying air temperature of 120°C, outlet drying air temperature of 60°C, and dryer duct height of 1.0 m. The total amount of water that exits the dryers was determined using the 10% desired water content of the exiting algae remains slurry.

3.5 Crude Lipid Extraction

Lipids released from the algae cells upon disruption must be extracted to produce biodiesel and lutein. This step is crucial in the manufacturing process, as lipids serve as the fundamental components of the end products. These algal lipids are rich in lutein fatty acid esters, which are used as the basis for free lutein powder. The structures of a triglyceride, a free fatty acid, and lutein fatty acid ester are featured in Figure 3-02. A comprehensive process flow diagram covering discussion sections 3.5 and 3.6 can be found in recommended design section 4.5.

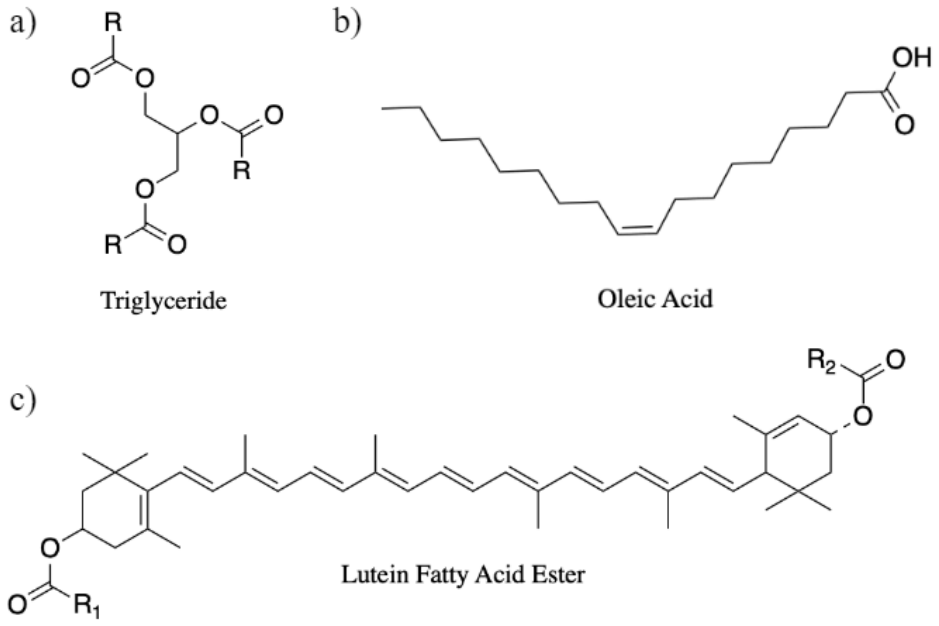

Figure 3.5-01: a) Triglyceride Structure; b) Free Fatty Acid Structure Example (Oleic Acid); c) Lutein Fatty Acid Ester Structure.

There are many different methods to extract lipids, including pressing, solvent extraction, supercritical fluid extraction, and ultrasonic-assisted extraction. Combining chemical and mechanical methods of extraction has been reported to increase efficiency (Mercer, 2011). The

previous bead milling step facilitates lipid extraction through mechanical cell disruption. Solvent extraction, a well-established approach, is suitable for scaling up to industrial levels. Chloroform and methanol will be introduced as solvents as suggested by Prommuak et al. The lipids will be highly soluble in the non-polar chloroform phase, and the cellular biomass will interact with the methanol phase. Solvents will be recovered and recycled to minimize waste, prevent solvent contamination, and reduce costs associated with solvent procurement.

3.5.1 Extraction with Chloroform and Methanol (R-201)

Chloroform and methanol are first mixed with the dried algae. The Bligh and Dyer method and the Folch protocol are the most common and practical methods of lipid extraction. In the Folch protocol, dried algae is combined with two volumes of chloroform and one volume of methanol (Eggers & Schwudke, 2016). In the Bligh and Dyer method, dried algae is mixed with one volume of chloroform and two volumes of methanol (Sündermann et al., 2016). Studies have indicated that the Bligh and Dyer method, accompanied by mechanical cell disruption, achieves the highest level of lipid extraction in *C. vulgaris* (Araujo et al., 2013; Moradi-kheibari et al., 2017). The Bligh and Dyer method additionally offers the advantage of requiring less chloroform, which minimizes potential toxicity to the nutraceutical. Prommuak et al. (2013) utilized a ratio of 60 mL solvent/g algae. As such, 22 million kg of chloroform and 23 million kg of methanol are needed per day. Research conducted by Moradi-kheibari et al. (2017) is used to determine lipid extraction yield. Using the Bligh and Dyer method, they obtained a total lipid yield of 38.57% based on dry biomass. Within the total lipids extracted, 53% consist of free fatty acids, or non-esterifiable lipids, while 47% are triglycerides, also called esterifiable lipids. Lutein fatty acid ester is additionally extracted in this step. Shi et al. (1997) determined the free lutein

content from *C. vulgaris* to be 3.1 mg free lutein/g algae. The amount of lutein fatty acid ester extracted was calculated to be 3360 kg/day assuming full conversion of lutein fatty acid ester into free lutein.

The design of the mixing tank is based on specifications provided by Portland Kettle Works. The dimensions are shown in Figure 3.5-02. The total height of the tank is 4.7 m. The total diameter of the tank is 2.7 m. There is a hydrodynamic pitched blade impeller operating at 300 rpm within the tank with three blades. Each blade has an outer diameter of 0.84 m. The motor system requires 5 HP, 400 V, and 8.5 FLA. The total capacity of the mixing tank is 6,354 gallons. The mixing tanks are operated at 90% capacity, following recommendations by Portland Kettle Works. It is assumed that the residence time of mixing is 10 minutes. As a result, 15 tanks are necessary to support the inlet flow of dried disrupted algae, chloroform, and methanol.

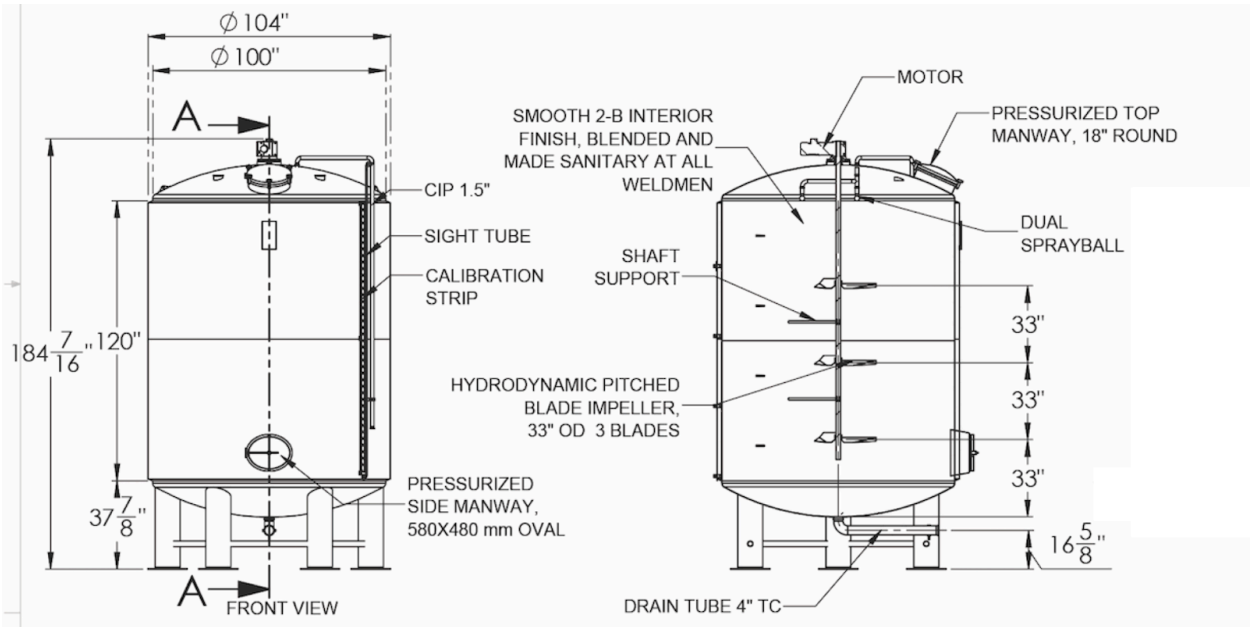

Figure 3.5-02: Lipid extraction mixer schematic (Portland Kettle Works, n.d.).

3.5.2 Centrifugation for Biomass Removal (R-202)

To address the cell debris, the lipid extract will be run through a disc stack centrifuge, specifically the MBUX 420 produced by Alfa Laval. Disc stack centrifugation, particularly, with jet-nozzle solids discharge, offers an efficient solid/liquid separation process that can run continuously. Centrifugation is based on the principle that components of different densities separate. As this process utilizes very large quantities of biomass, waiting for this separation to occur naturally in a setting pond would take too much time. Additionally the solids are the cells post-lysis, meaning that they are very small and so is their terminal velocity in solution. Spinning the solution increases the gravitational force that they experience, shortening the separation process significantly. The MBUX 420 offers the most capacity at 70L with a maximum throughput of 100 m^3/hr (MBUX, n.d.).

To determine volumetric flow, the terminal velocity,v_g, of the particles was found in meters/sec using (3-04a) where r_p is the radius of the particles (in meters and estimated as ¼ the radius of the original cells), ρ_p is the density of the particles was assumed using images from Hu (2014) as approximately four times the density of the individual pre-lysed cells (2300 kg/m^3), ρ_f is the density of the fluid (assuming a 50/50 methanol-chloroform solution with a weighted average density of 1123 kg/m^3), g is the acceleration due to gravity (m^2/s), and η is the viscosity of the fluid (also estimated as a weighted average, 0.006182 poise). This was then used in (3-04b) where Q is the volumetric flowrate through the centrifuge (m^3/s), n is the number of discs in the centrifuge, ω is the angular velocity of the centrifuge (rad/s), R_o is the outer radius of the centrifuge bowl (m), R_i is the inner radius of the bowl (m), and θ is the disc angle. With these conditions, 25 units operating at 25 L/s will be required to handle all of the solution exiting lipid extraction.

Solids will be discharged periodically at a weight percent of 94% which is high due to the intermittent nature of the discharge (time between discharges should allow for a more dense accumulation of solids) and can be tuned by the system. As chloroform made up a large percentage of the stream and was the next densest compound, it was assumed in the mass balance that the liquid lost would be primarily chloroform. This assumption makes the solids stream particularly hazardous, posing an environmental and safety threat. The stream must be treated and discharged as hazardous waste. The supernatant can then be sent for further separation.

$$v_g = \frac{4r_p^2(\rho_p - \rho_f)g}{18\eta} \tag{3-04a}$$

$$Q = \frac{v_g 2\pi(n-1)\omega^2}{3g} cot(\theta)[R_o^3 - R_i^3] \tag{3-04b}$$

3.6 Chloroform and Methanol Separation and Recovery

Due to the similar solvent properties of chloroform and methanol modification of the solvent mixture is required to create a phase separation. With the addition of water so as to achieve about equal masses of chloroform:methanol:water, a phase separation can occur between the organic chloroform phase and the aqueous methanol/water phase. In this instance, the desired components: free fatty acids and lipids will remain in the organic chloroform phase. Therefore, a decantation was chosen to separate the desired organic phase from the aqueous phase.

3.6.1 Post lipid-extraction solvent decanter (V-201)

The goal of this phase of the process was to separate the large amounts of methanol and chloroform from each other in the outlet stream of the disk stack centrifuge. To do this, liquid-liquid extraction was decided upon as a relatively cheap method that would preserve the lutein from heat based methods that would normally denature it.

Research into the liquid-liquid extraction of methanol and water from chloroform has been explored in the context of lipid extraction. This research identified a ratio of 1:1:0.9 (mass) mixture of chloroform, water, and methanol as optimal for separation according to Bligh and Dyer (1959). Given this, additional water was introduced to reach such levels prior to separation. Although this would increase the volume of materials processed, the resulting mixtures would provide two phases of near 100% purity in chloroform and water with methanol respectively.

To increase the speed at which the stream is processed, a centrifugal decanter was chosen over gravitational decanters. Additionally, extra constraints were put on the type of decanter chosen with emphasis on the ability to decant two liquid phases. Although different decanters exist that meet this purpose such as Flotwegg's tricanter series, ultimately the Alfa Laval Olive Oil X series was chosen due to the modularity of its design as well as the relative ease in acquiring decanters (Alfa Laval, n.d.; Flottweg, n.d.). From this series, in order to maximize the throughput of each unit, the maximum unit vessel size was prioritized. In doing so, the X9 variant was chosen as it was the largest in the series and the quantity of the decanters was scaled out to accommodate the massive total flow rate of the solvent mixture. In total, 284 units of this model of decanter were necessary to process all of the solvents in this step.

The performance of the decanting method used by Bligh and Dyer (1959) was modeled in Aspen Plus V14. The properties of chloroform, water, methanol, and any other chemicals

involved in this stage were modeled using Aspen's library of material properties. However, due to the lack of physical and thermodynamic properties for lutein esters in the Aspen Plus V14 database, lutein dipalmitate was inputted into the model as a user defined molecule and the Property Constant Estimation System (PCES) was used to automatically estimate the physical behavior of lutein dipalmitate in this phase separation. However, when errors occurred using PCES, it was assumed the lutein ester would behave similarly to a large non-polar molecule and remain dissolved in the organic chloroform phase. This assumption is not completely accurate due to entrainment phenomena that would occur inside a well-mixed binary phase system, but this phenomena was considered outside the scope of this project. Equilibrium conditions between water, methanol, and chloroform were modeled using NRTL correlations. The heavy outlet had a total flow rate of 859,000 kg/hr with a composition of 98.6% chloroform (by mass) with the remaining flow rate being triglycerides and 140 kg/hr of lutein. The light outlet had a total flow rate of 1,970,000 kg/hr with about equal parts water (47.6%) and methanol (49.1%) with only around 3.2% of the stream containing chloroform. These results were found using the optimal temperature and pressure of 20^{o} C and 1 atm.

3.6.2 Chloroform Evaporator (H-201)

The heavy phase from the solvent decanter is then flash evaporated to separate the desired lipids and free fatty acids from the toxic chloroform solvent. The evaporation of the chloroform from the lipid mixture was modeled using Aspen Plus V14. The evaporator was modeled as a flash drum and the operating temperature and pressure were varied to maximize the vaporization of chloroform. In the end, the evaporator operates at 120°C and 0.1 bar and low pressure steam provides the heat required to vaporize the chloroform. It is not necessary to

evaporate 100% of the chloroform due to the future use of chloroform for solvent separations in the first of two liquid-liquid extractions.

The vaporized chloroform is then recycled back to the crude lipid extraction reactor after getting condensed and being supplemented with a small makeup stream due to imperfect recovery. The liquid phase exiting the chloroform evaporator is then cooled to the necessary temperature for acid esterification. The chloroform vapor condenser and the crude lipid extract cooler were also modeled in Aspen Plus V14 as heater/cooler blocks using cooling water at Duplin county's yearly average dewpoint temperature of 17℃. Due to lack of experimental thermodynamic values for lutein fatty acid ester (modeled as lutein dipalmitate), the PCES system in Aspen Plus V14 was used to predict the separation of lutein ester molecules. However, when errors in the property estimation occurred, it was assumed that due to the comparatively large size of lutein ester molecules compared to the chloroform solvent, all of the lutein ester remained in the liquid phase.

3.6.3 Methanol and Water Distillation and Recycle (T-201)

To recover most of the methanol required for crude lipid extraction and water needed for decanting, a distillation column will be used to separate the methanol-water mixture leaving the decanter. Distillation was chosen for this operation due to its ability to achieve high enough purities required for solvent recycling. The light phase mixture is being fed to the column at 1,970,000 kg/hr with a composition of 47.6 wt% water, 49.1 wt% methanol, and 3.3 wt% chloroform. Due to chloroform's low boiling point, the fractional recovery of chloroform in the distillate is 100%. This distillation column was modeled in Aspen Plus as a RadFrac block

shown in Figure 3.6-01. The distillate is cooled to 20 C before being recycled back to the lipid extraction tank.

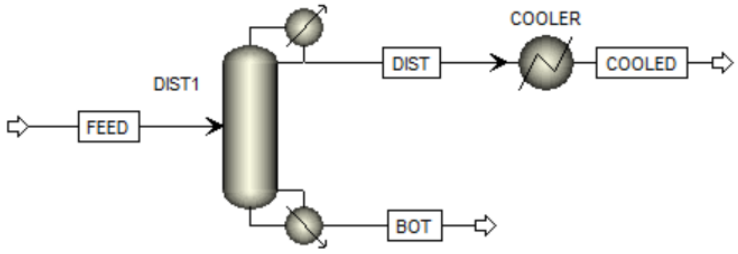

Figure 3.6-01: Aspen flowsheet for distillation modeling

A binary methanol-water xy diagram was generated using Aspen Plus. Phase equilibrium compositions were predicted with the NRTL correlation. A McCabe Thiele analysis was performed using the xy diagram to determine the reflux ratio, number of stages, and feed tray location. The minimum reflux ratio was estimated at $R_{min} = 0.79$ resulting in an operating reflux ratio of $R_{op}=1.18$ determined from the formula $R = 1.5R_{min}$. A total of 30 trays and a feed tray location above tray 22 was required to achieve water and methanol percent recoveries over 99.9%. To account for methanol lost in the bottoms product, a make-up stream will supply methanol to the distillate recycle. To avoid accumulation of water in the post lipid-extraction solvent decanter, the bottoms product will contain a purge stream that will send water with trace methanol to combine with the water feed later used in the chloroform/methanol/water liquid-liquid extraction.

3.7 Two-Step Transesterification and Saponification

280,000 kg lipids/day are harvested from the crude lipid extraction process. Microalgae lipids can be polar or nonpolar. Polar lipids include phosphoglycerides (phospholipids) and glycosylglycerides. Nonpolar lipids include triglycerides, free fatty acids (FFAs), sterols, acylglycerols, steryl esters, and waxes. The primary lipid source for biodiesel production is considered to be nonpolar lipids, predominantly triglycerides (Moradi-kheibari et al., 2017). Triglycerides consist of three fatty acid chains, with *C. vulgaris* predominantly featuring chains of either 16 or 18 carbons (Hu et al., 2008). Of the total lipids obtained, 130,000 kg/day are triglycerides suitable for transesterification into biodiesel, while the remaining lipids consist mainly of free fatty acids. Transesterification is most commonly facilitated by basic catalysts due to their ability to promote a rapid and controlled reaction. However, free fatty acids undergo a saponification reaction in the presence of an alkali catalyst. This results in partial consumption of the catalyst, lower biodiesel yield, and soap contamination (Vicente et al., 2004). The lipids will be pre-treated with an acid catalyst, converting the free fatty acids into esters before the introduction of the basic catalyst (El-Mashad et al., 2008). This step additionally increases biodiesel purity, ensuring compliance with the required ASTM D6751 acid value of 0.50 mg KOH/g, and reduces difficulties involved with separation of the final product (Rahman et al., 2017). Therefore, the production of biodiesel and free lutein will involve two steps: acid esterification and basic transesterification. A comprehensive process flow diagram covering discussion sections 3.7-3.10 can be found in recommended design section 4.6.

3.7.1 Acid Esterification (R-301)

FAME biodiesel can be synthesized through the acid esterification of free fatty acids (FFA) in the presence of sulfuric acid and methanol. The reaction is shown in figure 3.7-01.

Figure 3.7-01: Esterification of free fatty acids into FAME.

Rahman et al. (2017) found the optimal parameters for the acid esterification of *Spirulina maxima* to be a 12:1 molar ratio of methanol to oil, an acid catalyst concentration of 1wt%, a reaction temperature of 60˚C, a reaction time of 90 minutes, and a mixing intensity of 400 rpm. It is assumed that *C. vulgaris* will produce the same biodiesel yield as *Spirulina maxima* under these conditions. An average density of 0.87 kg/L and an average molecular weight of 273 g/mol were calculated for the FFAs based on the densities of linoleic acid, palmitic acid, and oleic acid (Ötleş & Pire, 2001). An average density of 0.895 kg/L and average molecular weight of 844 g/mol were calculated for the esterifiable lipids based on the triglycerides formed by linoleic acid, palmitic acid, and oleic acid. From the lipid extraction step, the total lipid yield is 280,000 kg/day. The non-esterified FFA lipid yield is 150,000 kg/day. The 12:1 molar ratio of methanol to lipids and the 1 wt% acid concentration reactor conditions described above result in a requirement of 272,000 kg methanol/day and 5,800 kg of 96% H_2SO_4/day for the acid esterification reaction. From the subsequent distillation column step, 228,000 kg/day methanol are recycled. Therefore, a make-up stream of 44,000 kg/day of methanol is required for the acid esterification reaction. As lutein exists as a fatty acid ester within the algae, it is assumed that it

is not affected by the esterification process. Additionally, under these conditions, the concentration of triglycerides is unchanged (Kail et al., 2012). Following assumptions outlined by Black et al. (2022) in their technical report, all of the FFAs react completely to produce FAME on a mass basis, resulting in 150,000 kg/day of FAME. However, the actual FAME yield should be slightly greater as FAME has a larger molecular weight than FFAs, although this discrepancy was not accounted for in the calculations.

Acid esterification occurs in a CSTR. The design of the CSTR is based on the geometric proportions of a "standard" agitation system proposed by Geankoplis et al. (2018) shown in Figure 3.7-02.

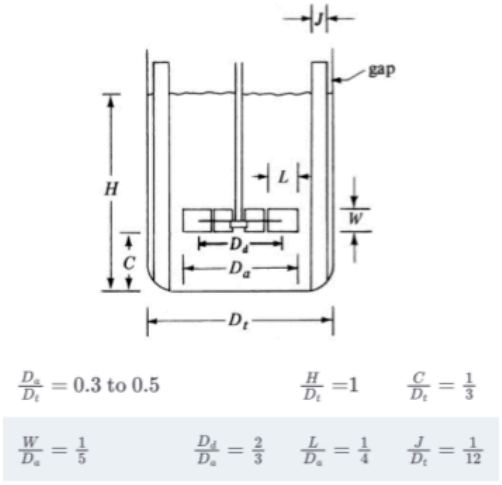

Figure 3.7-02: Dimensions of turbine and tank with geometric proportions for a "standard" agitation system (Geankoplis et al., 2018).

The total CSTR volume needed to support the total inlet flow rate based on a residence time of 90 minutes and the total inlet flow rate is 42 m^3. Three tanks were used to reduce individual tank sizing requirements. The diameter of the tank and the height of the liquid are 2.6 m. The total height of the tank is 3.0 m to account for additional head room. The impeller diameter is 0.87 m. The height of the impeller above the bottom of the tank is 0.87 m. The scaled-up impeller speed was calculated to be 48 rpm using methods from Geankopolis et al.

(2018), maintaining constant power per unit volume, as the reaction parameters from Rahman et al. (2017) were optimized for a one liter reactor.

3.8 Post Esterification Methanol Recovery and Acid Separation

The outlet stream exiting the acid esterification reactor contains triglycerides, FAME, methanol, chloroform, sulfuric acid, and water. The triglycerides and FAME must be separated from the methanol, chloroform, sulfuric acid, and water. This will involve a two step process consisting of a distillation column followed by a decanter. This was modeled in Aspen Plus using the NRTL base method. Sulfuric acid was not included in the components as it lacks NRTL parameters. It is therefore assumed that all of the sulfuric acid leaves the distillation column in the bottoms product and is completely separated from the lipids and FAME in the decanter. The process was modeled in Aspen Plus as shown in Figure 3.8-01. Triolein was chosen as the component to model the triglycerides. Methyl oleate was chosen as the component to model FAME.

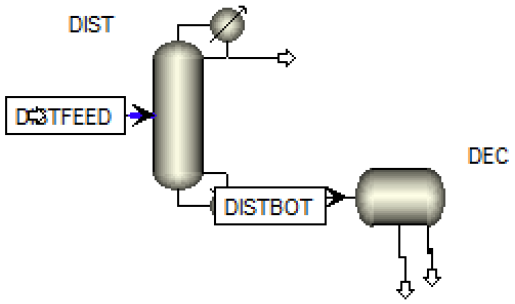

Figure 3.8-01: Acid esterification separations Aspen flowsheet

3.8.1 Acid Distillation Column (T-301)

The purpose of the acid distillation column is to recover and recycle most of the methanol back into the acid esterification reactor. The methanol is also removed to better facilitate the

phase separation in the decanter. The large flow rate of methanol can aid in the solubilization of various components, which can hinder the separation process. A total of 557,000 kg/day enters the column. The flow rate of methanol is 254,000 kg/day. 253,000 kg/day of methanol are able to be removed by the column in the distillate. The 792 kg/day of chloroform from the crude lipid extraction steps and 990 kg/day of water from acid esterification are additionally present in the distillate. A small purge stream of 10 percent of the distillate stream, or 25,500 kg/day will be present to prevent the buildup of chloroform in the acid esterification reactor. This stream contains 25,300 kg/day of methanol, 80 kg/day of chloroform, and 110 kg/day water and is sent to the first liquid-liquid extraction after base transesterification. Therefore 228,000 kg/day methanol will be provided to the acid esterification reactor from the distillate recycle stream. The bottoms product contains triglycerides, FAME, sulfuric acid, methanol, and water. The bottoms product is sent to a decanter to remove the sulfuric acid.

The distillation column was modeled in Aspen Plus. The distillate rate was set at 255,100 kg/day to maximize the amount of methanol in the tops product and the reflux ratio was set at 0.9. The distillation column contains 18 stages with the feed entering above tray 12. The column diameter is 1.9 meters and the total height is 9.75 meters.

3.8.2 Acid-Separation Decanter (V-302)

The acid-separation decanter was modeled in Aspen Plus V14. A total of 302,000 kg/day enters the decanter. This is separated into two different liquid streams that exit the decanter. One stream contains lipids and FAME. It consists of 133,000 kg/day of triglycerides, 150,000 kg/day of FAME, 200 kg/day of methanol, and 500 kg/day of water. The other stream contains water and

all of the sulfuric acid. It consists of 270 kg/day of methanol, 5,800 kg/day of H_2SO_4, and 8,100 kg/day of water.

The Olive Oil X9 decanter centrifuge manufactured by Alfa Laval, the same model as used in previous sections such as 3.6.1, was chosen due to the high volumetric throughput capabilities and its highly modular capabilities. Although this phase separation uses different solvents than the previous separations in which this decanter model was used, it was assumed that the modular capabilities of this decanter would be able to withstand any operating condition changes needed to successfully separate this new mixture. This was primarily done for ease of equipment sourcing and plant homogeneity, although experimental data to support this phase separation would have been more accurate.

3.8.3 Acid Neutralization (M-301)

The waste stream from the decanter contains sulfuric acid and must be neutralized. The acid will be neutralized using NaOH according to the following balanced equation shown by (3-05). 2 moles of base are required for each mole of acid. 4,000 kg/day of NaOH are needed to neutralize 5,800 kg/day of H_2SO_4. This reaction generates sodium sulfate and water and the resulting pH will be 7. The neutralized stream is assumed to be completely liquid due to the solubility of sodium salts in aqueous solutions and will be sent to municipal waste only once the pH is raised to acceptable levels.

$$2NaOH + H_2SO_4 \leftrightarrow Na_2SO_4 + 2H_2O \quad (3\text{-}05)$$

Similarly to acid esterification, the design of the mixer was calculated using the proportions of a “standard” agitation system proposed by Geankoplis et al. (2018) shown in Figure 3.7-02. The total tank volume required is 0.57 m^3 based on the total inlet flow rate into the

mixer and a residence time of 5 minutes. The tank has a diameter of 0.4 m and a liquid height of 0.4 m. A tank height of 0.5 m was chosen to account for additional head room. The diameter of the impeller is 0.13 m and it is positioned 0.13 m above the bottom of the tank. The impeller operates at 100 rpm.

3.9 Base Transesterification (R-302)

Biodiesel is also produced through the transesterification of triglycerides into FAME using methanol and an alkali catalyst (Meher et al., 2006). The reaction is shown in Figure 3.9-01.

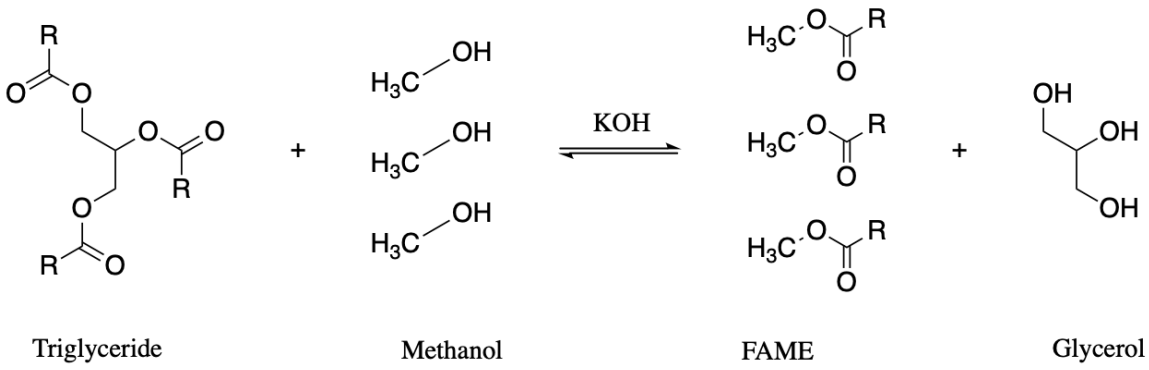

Figure 3.9-01: Transesterification of triglycerides into FAME.

Rahman et al. (2017) optimized the parameters of the transesterification of triglycerides derived from *Spirulina maxima* to include a 9:1 molar ratio of methanol to oil, a basic catalyst concentration of 0.75% (by weight), a reaction temperature of 65˚C, a reaction time of 20 minutes, and a mixing intensity of 600 rpm. Similarly to the acid esterification step, it is assumed that *C. vulgaris* will exhibit the same reaction behavior as *Spirulina maxima*, and calculations were conducted using the average density and molecular weight of the esterifiable and non-esterifiable lipids. Rahman et al. (2017) determined FAME yield to be 86.1% of the total lipid mass. 204,000 kg/day of methanol are needed. This methanol is recycled from a distillation

column that follows the first liquid-liquid extraction step. With an inlet flow rate of 280,000 kg total lipids/day, 244,000 kg/day of FAME will be produced from both acid esterification and transesterification. Assuming complete conversion of all FFAs into FAME, 94,000 kg/day of triglycerides react to produce FAME in order to accomplish the 86.1% yield. From lipid extraction, the esterifiable lipid yield was 133,000 kg/day. This indicates a 70% conversion of triglycerides. These transesterification conditions were additionally deemed suitable for the simultaneous saponification reaction of lutein fatty acid ester into free lutein (Prommuak et al., 2013). The reaction is shown in Figure 3.9-02. It is assumed that all of the lutein fatty acid ester is saponified to produce the desired free lutein compound and soap. This results in a total of 1,800 kg free lutein/day.

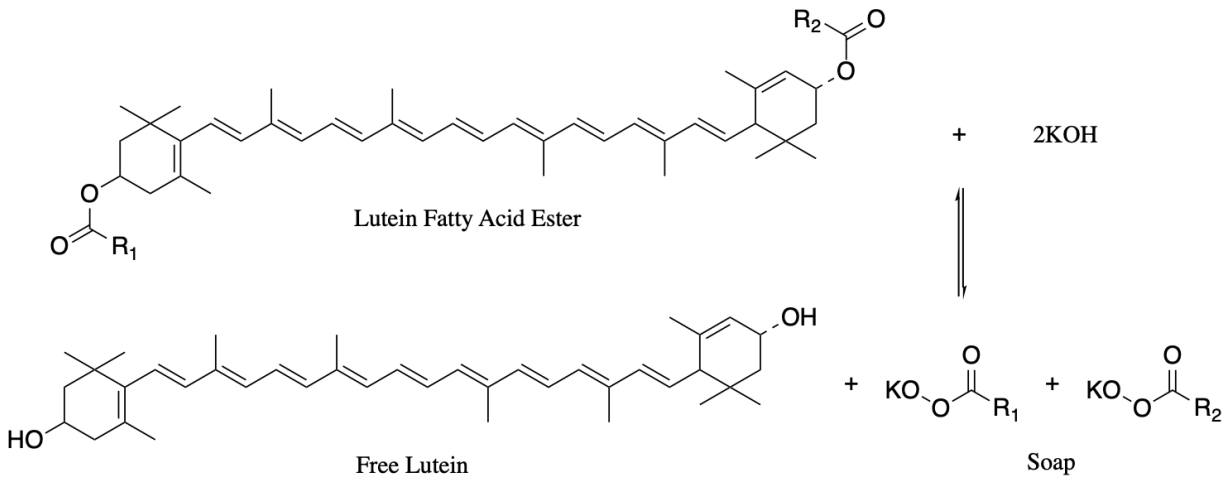

Figure 3.9-02: Saponification of lutein fatty acid ester into free lutein and soap.

The design of the CSTR for base transesterification was calculated using the proportions of a "standard" agitation system proposed by Geankoplis et al. (2018) shown in Figure 3.7-02. The total CSTR volume needed to support the inlet flow rate based on a residence time of 20 minutes is 8 m^3. One tank was used. The diameter of the tank and the height of the liquid are 2.2

m. The total height of the tank is 3.5 m to account for additional head room. The impeller diameter is 0.72 m. The height of the impeller above the bottom of the tank is 0.72 m. The scaled-up impeller speed was calculated to be 81 RPM using methods from Geankopolis et al. (2018), maintaining constant power per unit volume, as the reaction parameters from Rahman et al. (2017) were optimized for a one liter reactor.

3.10 Chloroform/Methanol/Water (CMW) Liquid-Liquid Extraction and Solvent Recovery

A very similar process to the one outlined in section 3.6.1 will serve as the method for separating solvents from the FAME and Lutein products produced in the previous esterification reactions. Following extraction of these products in the heavier organic phase consisting mostly of chloroform, a distillation column and flash process will be used to separate and recover methanol from the aqueous mixture in this decanting process.

3.10.1 CMW Liquid-Liquid Extraction Design Considerations (V-303)

Following the simultaneous transesterification and saponification reactions, chloroform is added in line to dissolve the FAME biodiesel and free lutein as well as any unreacted glycerides. Prommuak et al. (2013) specifies a volume ratio of 10:10:9 of chloroform:mixture:water with the addition of centrifugation to achieve the separation of the upper methanol/water phase containing potassium hydroxide, glycerol, and soap from the lower chloroform phase with biodiesel, lutein, and unreacted glycerides.

Assumptions are made about the distribution of soap and lutein across the two output streams. Soap is assumed to be aqueous being divided in identical proportions to the water distribution across both streams. Similarly, chloroform serving as a solvent for lutein provides a proportion of lutein in each stream equal to its own distribution.

Operations for this process were simulated using a combination of Aspen Plus V14 NRTL based modeling and parameters such as vessel volume (0.575m in diameter and 2.44m in length) for the Alfa Laval X9 Olive Oil decanter in three phase configuration. The choice of decanter originates for the same reasons that this type of decanter was chosen for section 3.6.1. Operational pressure was determined to be optimal at 1 atm given the minimal effect found when varied between 1-10 atm. Sensitivity studies showed at 20^{o}C, purity for the heavy stream (in terms of chloroform) was preserved while maximizing throughput. This combination of parameters yields a heavy stream totalling 859,000 kg/hr of which 98.6% is Chloroform by mass with the remaining composition being triglycerides (1.3%) and lutein. In comparison the light stream has a flow rate of about 1,970,000 kg/hr with only 3.2% Chloroform by mass with the remaining composition being roughly equal parts methanol (49.1%) and water (47.6%) by mass.

3.10.2 Methanol/Water Distillation Column (T-302)

Following the separation of the chloroform phase from the aqueous methanol and water phase through decantation, a distillation column is used to separate the methanol from the water. 214,000 kg/day of methanol is present in the light phase exiting the decanters which can be recycled to the base transesterification reactor. The first step in the process involves separating the copious amounts of water from this stream. To do this, a distillation column modeled in Aspen Plus separates the methanol and chloroform due to their similar boiling points from the water and other heavy components present (FAME, glycerol, lutein, KOH, triglycerides, and some trace amounts of methanol and chloroform). The bottoms product containing water and all of the glycerol and soap is discarded as waste, while the distillate consisting of methanol, chloroform, and some water is sent for further separation. The glycerol could be further

separated and sold, but that was deemed out of scope and would not provide a very lucrative revenue stream.

3.10.3 Methanol/Chloroform Distillation Column (T-303)

A specific column is required for methanol and chloroform due to their similar boiling points, so a second distillation column is utilized to remove the chloroform in order to recycle the methanol back into the base transesterification reaction. The distillation column was modeled using Aspen Plus. The distillation column contains 20 stages, and the feed enters above stage 10. The reflux ratio was set to 11 on a mass basis and the distillate rate was set at 77,500 kg/day to remove as much chloroform as possible. The diameter of the column is 1.6 m and the height is 10.97 m. This process additionally ensures that the required amount of methanol is entering base transesterification. The bottoms product contains mainly methanol whereas the distillate is primarily chloroform. The chloroform is considered a waste stream, however it could be beneficial to recycle it into previous unit operations to slightly reduce costs.

3.10.4 Solvent flash (H-301)

After the organic (mostly chloroform) phase is decanted off from the aqueous methanol phase in the chloroform/methanol/water liquid-liquid extraction (section 3.10.1), the undesired solvents must once again be evaporated off from the products. This time however, there is some methanol and water present with a majority of chloroform and it is more important than the previous chloroform flash that as much chloroform be evaporated off as possible due to the lack of further unit operations downstream using chloroform for solvent separations. This flash was modeled in the same way as the chloroform evaporator described in section 3.6.2, however, the temperature was raised to 135 C to improve the separation of chloroform from the desired

biodiesel and lutein products. This was not expected to have a great deal of effect on the degradation of lutein since the temperature was only raised 15 degrees, however further experimentation into the degradation of lutein at higher temperatures may contradict this. As a result, instead of using low pressure steam as the utility providing heat through heating coils, medium pressure steam was required to achieve this higher temperature. In addition, a chloroform condenser was modeled using a heater block with cooling water as the heat sink. The FAME and lutein product stream with trace amounts of glycerol, KOH, unreacted triglycerides, and chloroform was also cooled using a heater block in aspen with cooling water as the heat sink. The final temperature of the product stream however is 20°C instead of 60°C, as it was for the first chloroform flash, because this is the optimal temperature for the subsequent liquid-liquid extraction with ethanol/hexane/water. Once again, the PCES was used to model the separation of lutein between the vapor and liquid phases, and if errors occurred, it was assumed that all of the lutein remained in the liquid phase due to its large molecular size in comparison to the chloroform solvent.

3.11 Hexane/Ethanol/Water (HEW) Liquid-Liquid Extraction

Another liquid-liquid extraction, this time using hexane and aqueous ethanol as the solvents, will serve as the method for separating lutein from FAME once most of the chloroform in the solution containing both these chemicals has been removed through the evaporator found in the previous section, 3.10.4 Solvent Flash. A comprehensive process flow diagram covering discussion sections 3.11-3.13 can be found in recommended design section 4.8.

3.11.1 HEW Liquid-Liquid Extraction Design Considerations (V-401)

The solvents used in this operation vary from what was used in previous extractions with aqueous ethanol replacing chloroform as the solvent for lutein and hexane being used for the FAME extraction. This was recommended by the research of Gong et al. (2018), in their paper exploring the simultaneous extraction of lutein and lipids from similar algae. This phase separation was modeled in Aspen Plus V14 using NRTL correlations. Once again, for the lutein molecules in solution, PCES was used to predict their separation behavior between phases, but if PCES ever produced errors, it was assumed that the lutein remained completely dissolved in the ethanol phase due to the presence of hydroxyl groups that can form hydrogen bonds with the solvent. Although no particular ratio between the two solvents was provided by Gong et al. (2018), ultimately, through trial and error during the modeling process, a 1.43:1 hexane to ethanol ratio (by mass) was found to be optimal for the separations necessary. A similar assumption used in both previous uses of decanting was employed with proportional amounts of the dissolved substances being found in each stream equal to the proportion of their solvents in said streams. As with other decanting models, operational temperatures between 20-25^{o}C were found to be optimal for phase separation. The operational pressure in the model was found to have minimal impact on the outcome of the product as such, it was best left at 1.0 bar.

Similar to the rest of the decanting operations used throughout the whole process, Alfa Laval's X9 Olive Oil decanters were chosen to perform this separation due to their high through-put capabilities, ability to operate at the specified temperature and pressures listed above, and their high modular capabilities. Due to the flow rate required for processing, the number of these decanter units was once again scaled out to a total of only 2 required units to

fulfill throughput requirements. The final design specifications of these units can be found in section 4.8.1.

3.12 Lutein Crystallization and Filtration (M-401, V-401)

The light phase out of Hexane/Ethanol/Water Liquid-Liquid Extraction consisting primarily of ethanol also contains the dissolved lutein. As the intended product is a crystalline powder, a crystallization step is required. Supercritical CO_2 in an anti-solvent process can be used for high-yield precipitation of lutein (Miguel et al., 2008). This process however is quite extensive (and expensive), involving the addition of a handful of unit operations, which was considered too complex for the scope of this design project. Vacuum filtration was also considered, but because the temperatures needed to vaporize the ethanol surpassed the degradation temperature of lutein even with a pressure of 0.1bar. Prommuak et al. (2013) had suggested an antisolvent process using water but did not conduct experiments to study this. Vechpanich and Shotipruk (2013) found that adding water to ethanol in a 4:1 ratio with 30 minutes of agitation resulted in a 99% yield of lutein. As this process did not require the addition of heat and was fairly inexpensive, it was determined to be the most viable option. With this method, water is added to the ethanol phase exiting the hexane/ethanol liquid-liquid extraction decanter in a crystallizer unit that agitates the solution. The crystals are then collected by passing the exiting stream through a membrane filter and periodically clearing the filter. The crystals can then air-dry before transport. The crystal-free solution would then require two distillation columns to yield pure ethanol and eliminate the large quantity of water and trace contaminants. This was deemed out-of-scope for this project, so the solution was treated as hazardous waste.

3.13 FAME Biodiesel Purification (T-401)

The hexane phase exiting the hexane/ethanol liquid-liquid extraction decanters contains hexane and the FAME product with traces of triglycerides, water, chloroform, glycerol, lutein, and ethanol. Hexane cannot be present in the final product, and there are strict guidelines on specific components and their amounts in the finished biodiesel. As FAME has a very high boiling point, the most efficient method of separation is a distillation column. The column can operate at relatively high temperatures to ensure an essentially pure product. As the distillate contains a large amount of hexane, it would be advantageous to recycle the stream. It also contains some contaminants like chloroform which would need to be purged to prevent accumulation in the process, but this step would require a second distillation column that was out of scope for the purpose of this plant, so the stream is treated as hazardous waste.

4. Recommended Design

4.1 Algae Cultivation

An overview of the algae cultivation process and subsequent algae harvesting steps are performed in Process Section 1 shown in Figure 4.1-01. Swine waste serving as the algae nutrient source is mixed into water in the raceway pre-mixing tank (M-101) before being sent to the raceway ponds (R-101). Harvested algae is concentrated in the dissolved air floatation (DAF) unit (V-101, V-102, C-101). Algae concentrate is sent to the bead mill unit (M-102, R-102) for cell disruption. The disrupted algae mixture is dried to a biomass paste in a cross-flow dryer (H-101) before being sent to the lipid extraction process section.

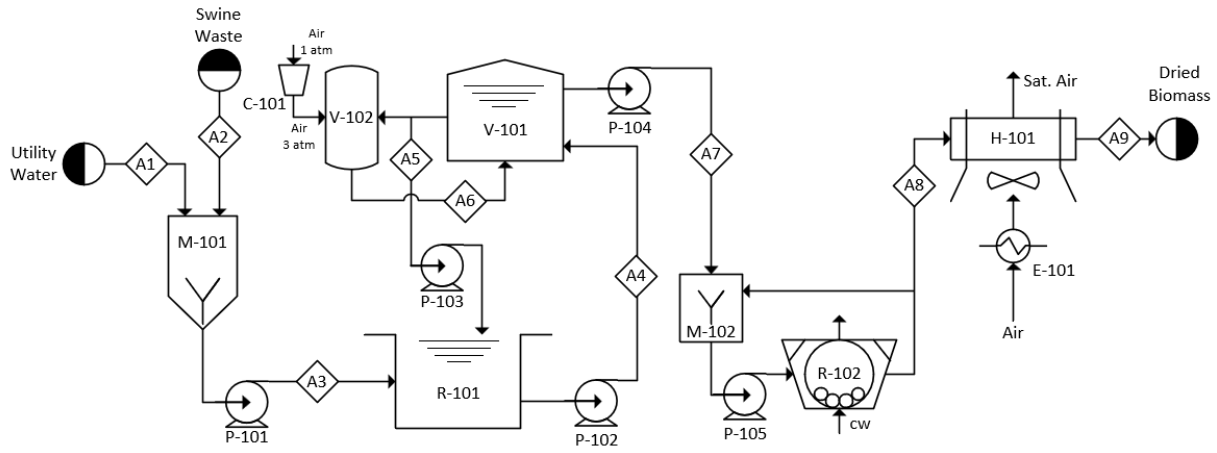

Figure 4.1-01: Process Section 1 - Algae cultivation and harvesting

4.1.1 Pre-mix Tank (M-101)

Tanks trucks unload pig waste into the pre-mix tank which is a vertical cylindrical vessel 8.5 meters tall, with a diameter of 8.5 meters. Supplemental water also flows at 9.78M kg/day into the tank. An exiting stream of water and waste (A3) is then pumped into the batch of 216 raceways at 13.74M kg/day mixing with the recycled water from DAF containing algae that seeds the raceways. A different batch is refilled each day.

4.1.2 Raceways (R-101)

The raceways are then filled with the recycled water from DAF and the slurry from the premix tank. They are constructed using compact gravel and a UV-resistant PVC liner. The raceways are configured with 1 meter-wide walkways between each for maintenance as shown in Figure 4.2-02. There are 20 columns of 216 raceways resulting in 4,321 raceways in total with a footprint of 1.04 km^2. A 14’ diameter paddle wheel, made out of steel and powered by a 2 HP motor, rotates at 20 rpm in each raceway to provide turbulent conditions throughout the growth period. After 20 days, the solution is pumped out to Dissolved Air Flocculation. This process is outlined in Table 4.1-01 which shows the average flows on a given day comprising multiple different batch operations.

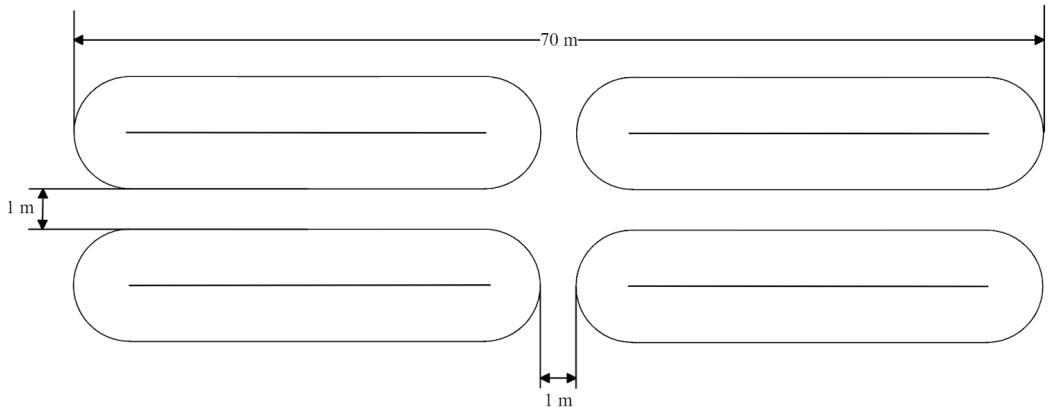

Figure 4.1-02: Raceway layout schematic

Table 4.1-01
Algae Cultivation Stream Table

Streams (kg/day)*	**A1**	**A2**	**A3**	**A4**	**A5**
Biomass	0	0	0	833,333	75,000
Water	10,539,307	0	10,539,307	83,333,333	69,594,445
Pig Waste**	0	3,957,914	3,957,914	-	-

*Daily average flows spread across the many batch processes of algae cultivation
**Pig waste is accounted for in the algae biomass and assumed to be in dilute concentration in the DAF water stream.

4.2 Dissolved Air Flotation System

The dissolved air floatation (DAF) process is composed of three main operations, the DAF vessel unit (V-101), the saturator tanks (V-102), and air compressors (C-101). Recommended design of each unit is discussed below.

4.2.1 DAF Units (V-101)

Ecologix Environmental Systems provides industrial-sized DAF units. Specifications for the E-1035 model are used. The maximum allowable flowrate through the system is 735.1 m^3/h. As a result, 5 DAF units are utilized to accommodate the 3,500 m^3/h flowrate of algae solution. The E-1035 is 13.2 m in length, 3.4 m in width, and 3.3 m in height. The surface area covered by one unit is 469.9 m^2.

4.2.2 Saturator Tanks (V-102)

The built-in saturators (V-102) in the E-1035 models require a total of 1.9 million kg/day of air-saturated water. The DAF units have a recycle stream of water directed back into the

saturator to be utilized as the source of water for air saturation. This ensures a continuous supply for the saturator and eliminates the need for an additional water stream, reducing costs. Additionally, the rest of the water, around 70 million kg/day, will be recycled back into the raceways, serving to reduce water requirements and acting as an inoculant for the algae cultivation process.

4.2.3 Air Compressor (C-101)

An air compressor supplies pressurized air at 3 atm to the saturator tank. The unit was modeled in Aspen Plus to determine the flow rate of hot air after pressurization occurs. An inlet air stream at ambient temperature was varied to satisfy the calculated outlet air flow rate of 133.8 m^3/day necessary to saturate the water in the saturator tank. The resulting ambient air flow into the compressor is 11 m^3/hr to produce 5.58 m^3/hr of air at 3 atm. The brake horsepower of the compressor was reported to be 0.56 kW. The flow rates entering and exiting the DAF units are shown in Table 4.2-01.

Table 4.2-01
DAF Stream Table

Streams (kg/day)	**A4**	**A5**	**A6**	**A7**
Biomass	833,333	75,000	0	758,333
Water	83,333,333	69,594,445	1,858,333	11,880,556
Air	0	0	126	0

4.3 Bead Milling Process

The bead milling process consists of 200 bead mills and 20 feed tanks arranged in parallel. Figure 4.3-01 shows the process flow diagram for the bead milling process. A single

feed tank supplies the algae suspension for 10 bead mills. Flow rates of disrupted biomass is shown in Table 4.3-01.

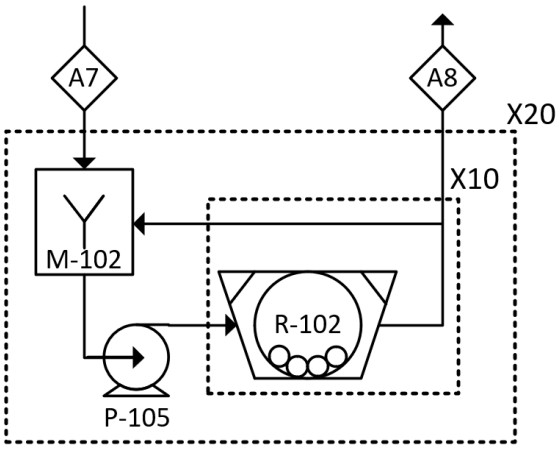

Figure 4.3-01: Bead mill process flow diagram showing distribution of tanks and mills

Table 4.3-01
Bead Milling Stream Table

Streams (kg/day)	**A7**	**A8**
Biomass	758,333	166,833
Disrupted Biomass	0	567,840
Water	11,880,556	11,904,216

4.3.1 Bead Mill Feed Tanks (M-102)

The bead mill feed tanks are 1200 L vessels made from 316 SS with a height and width of 1.15 meters. The feed tanks have a working volume of 1000 L. The tanks are supplied with concentrated algae from stream A7 at a rate of 7 L/s. Each tank is equipped with a feed pump (P-105) to supply 40 L/s of algae feed to its unit of 10 bead mills. The recycle line supplies 33

L/s of disrupted cell suspension back to a single feed tank to maintain constant volume while the remaining 7 L/s leaves the process in stream A8. Each feed tank is equipped with a 4-blade axial impeller made from 316SS. The impeller has a diameter of 15 inches and a speed of 130 rpm. The required power to drive a single impeller at this speed is 526W.

4.3.2 Bead Mills (R-102)

The DYNO-MILL ECM-AP 60 is used as the bead mill for this process due to its ability to support beads sizes greater than 0.10 mm and its incorporated DYNO-ACCELERATOR DSE agitator design that was used in lab-scale mills to produce the data reported by Postma et al. (2017) and Suarez-Garcia et al. (2019). The working volume of the bead mill is 62 L. Each bead mill is operated with a throughput of 4.0 L/s and an accelerator speed of 400 rad/s. The bead mills are filled with 0.40 mm diameter Tosoh YTZ beads at 65% fill ratio based on volume. The resulting power consumption of a single bead mill is 132 kW and the cooling water throughput is 4000 L/hr (WAB Group, n.d.).

4.4 Biomass Drying (H-101)

The inlet solution to the dryer contains 6% algae (by weight). The objective of the conveyor belt dryer is to further dry the solution to 90% algae (by weight) in order to achieve efficient and effective lipid extraction. The bed width is 3 m, the bed length is 39 m, and the material depth is 0.05 m. The residence time will be 311.42 minutes. 2,161 dryers are needed to accommodate the large quantity of algae solution being processed each day. 1,700 cubic meters/second of hot air entering the system at 120˚C are required to reach an outlet water flow rate of 81,000 kg/day, corresponding to 90% algae (by weight). 86,000 kW of energy are used in a boiler to heat 71,000 cubic meters/day of air at 25˚C to produce the volume of air at 120˚C.

Hot air enters the conveyor belt dryers through a circular vent. Each dryer receives 0.79 m^3/sec of hot air. The air is blown at a velocity of 1 m/s. This velocity ensures dry algae is not dispersing and floating uncontrollably within the system. The cross sectional area of the vent is 0.79 m^2, corresponding to a vent radius of 0.5 m. The inlet and outlet streams are shown in Table 4.4-01.

Table 4.4-01
Cross Flow Dryer Stream Table

Streams (kg/day)	**A8**	**A9**	**Dryer Air Inlet**	**Dryer Air Outlet**
Biomass	166,833	166,833	0	0
Disrupted Biomass	567,840	567,840	0	0
Water	11,904,216	81,630	0	11,822,586
Air	0	0	$1.2x10^8$	$1.2x10^8$

4.5 Crude Lipid Extraction

The crude lipid extraction process will take place in a continuous stirred tank (R-201). The crude lipid extract will undergo a series of separations using a disk stack centrifuge (R-202), a decanter (V-201), a water methanol distillation column (T-201), and a chloroform flash drum (H-201). Figure 4.5-01 provides an overview of the lipid extraction in Process Section 2.

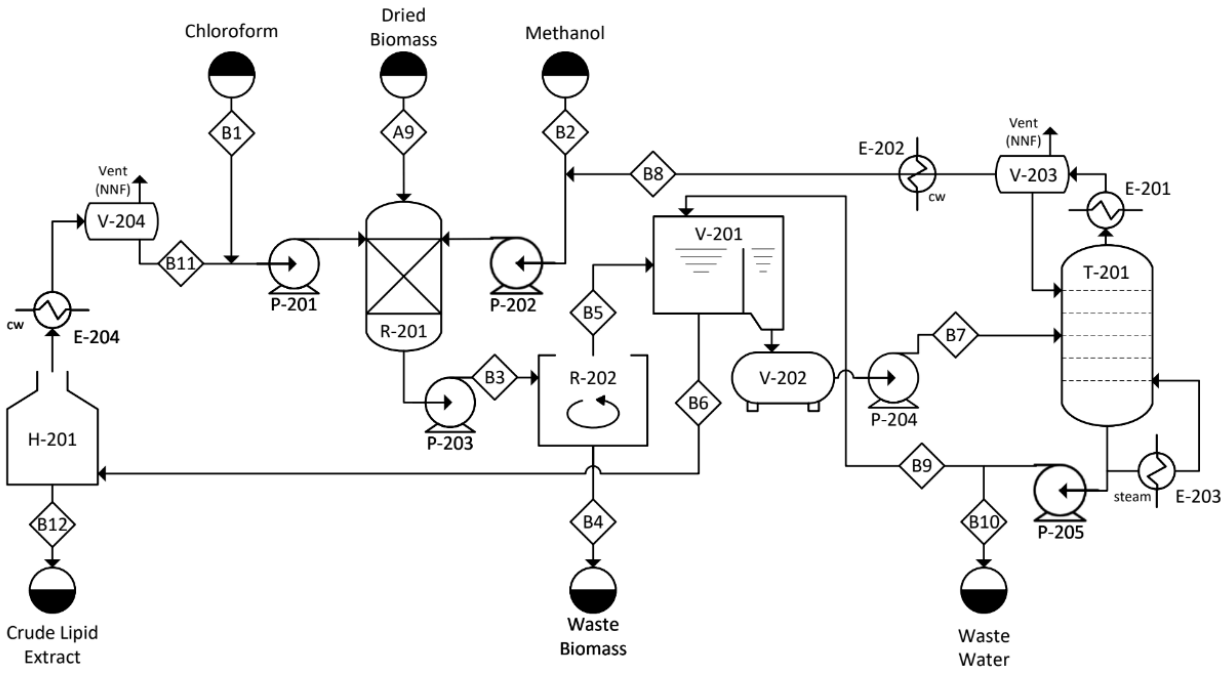

Figure 4.5-01: Process Section 2 - Crude lipid extraction

4.5.1 Crude Lipid Extraction Mixer (R-201)

15 mixing tanks from Portland Kettle Works are utilized to combine 22 million kg of chloroform and 23 million kg of methanol with 735,000 kg of biomass per day. The tank is 4.7 m in height, 2.7 m in diameter, and contains a hydrodynamic pitched blade impeller operating at 300 rpm within the tank with three blades. Each blade has an outer diameter of 0.84 m. The residence time is 10 minutes. A daily production of 283,000 kg/day of lipids is achieved. 133,000 kg/day consist of triglycerides and 150,000 kg/day are FFAs.

Table 4.5-01
Crude Lipid Extraction Stream Table

Streams (kg/day)	A9	B1	B2	B3	B8	B11
Biomass*	734,673	0	0	447,936	0	0
Chloroform	0	29,592	0	21,893,256	1,530,504	20,333,160
Methanol	0	0	48	23,274,456	23,274,408	0
Water	81,630	0	0	87,720	6,090	0
Lipids**	0	0	0	283,368	0	0
Lutein Ester	0	0	0	3,360	0	0

*Contains both disrupted and intact algal biomass
**Contains both triglycerides and free fatty acids

4.5.2 Disc-stack Centrifuge (R-202)

Immediately post crude lipid extraction, the MBUX 420 disc-stack centrifuge from Alfa Laval spins down the cell debris to remove it as a waste stream. The MBUX 420 has a capacity of 70L, spins at 3740 rpm, and can support a throughput of 25L/s for this process. With this throughput, 25 units are required to remove all of the cell debris. Overall, the debris is removed at 3447,936 kg/day along with 28,800 kg/hr of chloroform. A summary of component flow rates are shown in Table 4.5-02.

Table 4.5-02
Disc-stack Centrifuge Stream Table

Streams (kg/day)	B3	B4	B5
Biomass*	447,936	447,936	0
Chloroform	21,893,256	28,800	21,864,456
Methanol	23,274,456	0	23,274,456
Water	87,720	0	87,720
Lipids**	283,368	0	283,368
Lutein Ester	3,360	0	3,360

*contains both disrupted and intact algal biomass
**contains both triglycerides and free fatty acids

4.5.3 Post Lipid-Extraction Solvent Decanter and Holdup Tank (V-201 and V-202)

A total of 284 decanters are operated to separate a solution meeting the specifications discussed in section 3.6.1. To induce phase separation, a total of approximately 22,500,000 kg/day of water is mixed with the chloroform/methanol mixture in the decanters. The decanters for this operation are the aforementioned Alfa Laval X9 olive oil decanters as a result of their high throughput and ability to be modified into 'tricanters' capable of separating a solid, heavy phase, and light phase from each other (Alfa Laval Inc., n.d.). Each decanter has a circular vessel sized at 575 mm in diameter and 2440 mm in length. This bowl/vessel is designed to be spun at 2900 rpm (Alfa Laval, n.d.; Flottweg, n.d.). As a result, this separation results in a heavy phase (B6) primarily composed of chloroform (approximately 98% by weight), with lipids and a very small amount of lutein by mass. Most of the 3,360 kg/day of lutein esters in the B5 inlet are split into the heavy phase with a negligible amount being lost in the light phase.

Table 4.5-03
Lipid Decanter Stream Table

Streams (kg/day)	B5	B6	B7	B9
Chloroform	21,864,456	20,333,952	1,530,504	0
Methanol	23,274,456	0	23,286,336	11,880
Water	87,720	0	22,569,456	22,481,736
Lipids*	283,368	283,368	0	0
Lutein Ester	3,360	3,360	0	0

*contains both triglycerides and free fatty acids

4.5.4 Water and Methanol Distillation Column (T-201)

In total, 20 columns make up distillation unit T-201. Each column is 17.1 m in height and 4.27 m in diameter resulting in a height to width ratio of 4:1. There are a total of 28 sieve trays with the feed entering above tray 22 where tray 1 is located at the top of the column. The column feed enters at 20°C and the distillate and bottoms product streams leave at 63.1°C and 99.9°C respectively. The columns are equipped with a total condenser operated with a reflux ratio of 1.18 and a heat duty of -33,000 kW; the condenser is supplied with cooling water at 17°C. The reboiler design is a partial kettle reboiler with a boil-up ratio of 1.0 and a heat duty of 40,300 kW; the reboiler is heated with low pressure steam at 125°C.

Single column flow rates are as follows: the feed flow rate is 2,369,000 kg/day containing 47.6 wt% water, 49.1 wt% methanol, and 3.30 wt% chloroform; the distillate flow rate is 1,241,000 kg/day containing 0.020 wt% water, 93.81 wt% methanol, and 6.17 wt% chloroform; the bottoms product flow rate is 1,128,000 kg/day containing 99.95 wt% water, 0.05 wt% methanol, and 0.0 wt% chloroform. The bottoms product is split into streams B9 and B10 such

that the material balance around the lipid decanter V-201 is maintained. A summary of the total component flow rates leaving the distillation system is shown in Table 4.5-04.

Table 4.5-04
Distillation (T-201) Stream Table

Streams (kg/day)	**B7**	**B8**	**B9**	**B10**
Chloroform	1,530,504	1,530,504	0	0
Methanol	23,286,336	23,274,408	11,880	48
Water	22,569,456	6,090	22,481,736	81,630

4.5.5 Chloroform Flash Drum (H-201)

The chloroform flash drum (H-201) operates at 120°C and 0.1 bar. The vessel is made of stainless steel and has a diameter of 14.9 m and a height of 3.66 m. The total volume of the tank is 640 m^3 and the heat duty provided by low pressure steam through heating coils is 77 MW. To pull vacuum in the vessel, 52 kW of electricity are used by a compressor to achieve 0.1 bar. The total inlet and outlet flow rates are shown in Table 4.5-05.

Table 4.5-05
Chloroform Evaporator Stream Table

Streams (kg/day)	**B6**	**B11**	**B12**
Chloroform	20,333,952	20,333,160	792
Lipids*	283,368	0	283,368
Lutein ester	3,360	0	3,360

*Contains both triglycerides and free fatty acids

4.6 Two Step Transesterification and Saponification

The production of FAME and lutein involves an acid esterification reactor (R-301), a methanol recovery distillation column (T-301), an acid separation decanter (V-302), an acid neutralization step (M-301), a base transesterification reactor (R-302), a chloroform recovery evaporator (H-301), CMW liquid-liquid extraction (V-303), a methanol water distillation column (T-302), and a methanol chloroform distillation column (T-303). Figure 4.6 provides an overview of the lipid esterification and solvent separation processes in Process Section 3.

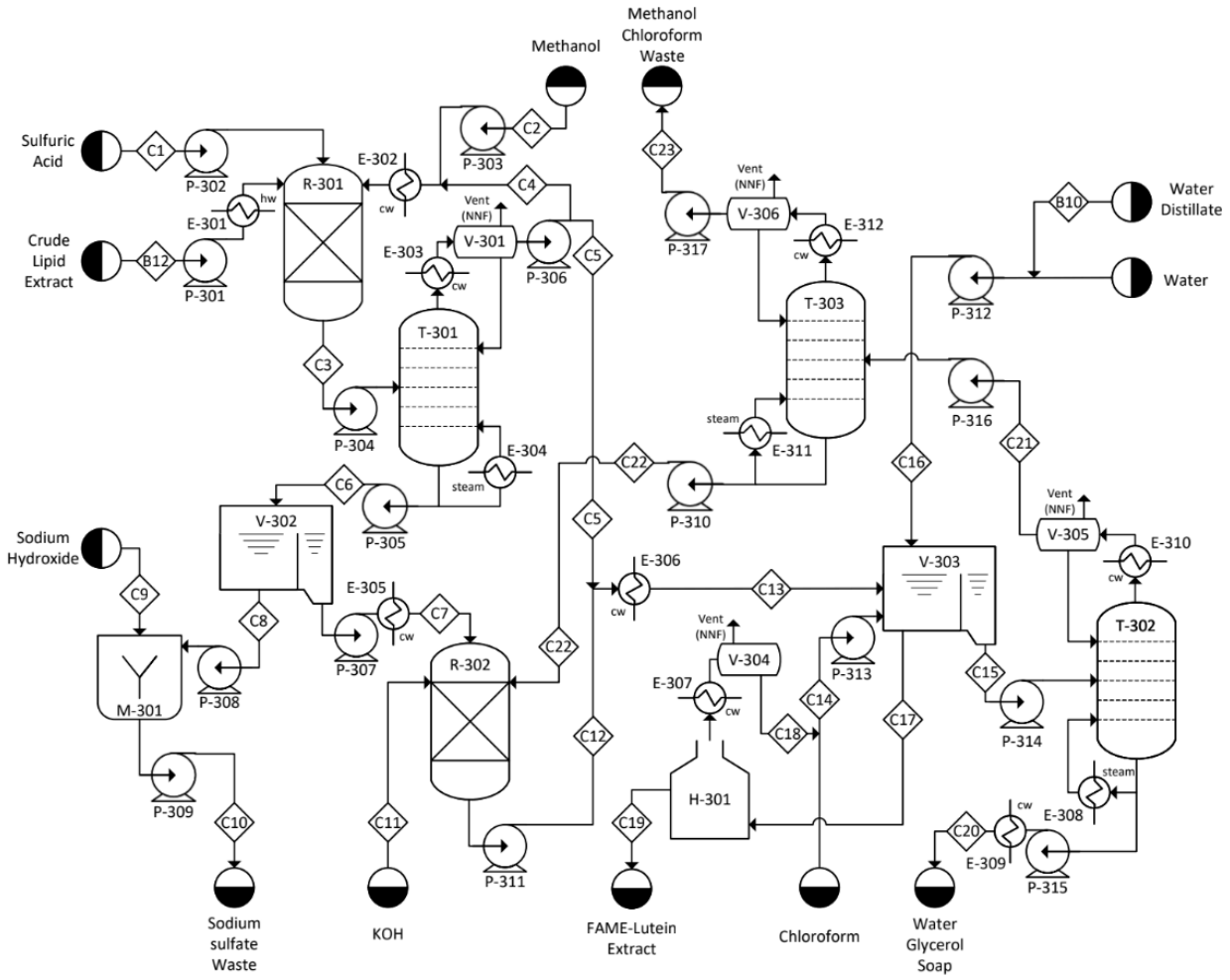

Figure 4.6-01. Process Section 3 - Lipid esterification and solvent separations.

4.6.1 Acid Esterification (R-301)

The acid esterification reaction occurs at 60˚C with a residence time of 90 minutes. The total inlet flow rate into acid esterification is 567,000 kg/day. 150,000 kg/day of FAME are produced in the acid esterification step. 18,000 kg/day of methanol are consumed in the reaction. 9,900 kg/day of water are produced. Three CSTR units are used, with a tank height of 3.0 m and diameter of 2.6 m. The impeller diameter is 0.87 m and it operates at 48 rpm. The streams entering and exiting the acid esterification unit are shown in Table 4.6-01.

Table 4.6-01
Acid Esterification Stream Table

Streams (kg/day)	**B12**	**C1**	**C2**	**C3**	**C4**
Methanol	0	0	43,778	254,082	227,890
Chloroform	792	0	0	792	713
Water	0	0	0	9,892	988
FFA	150,094	0	0	0	0
Triglyceride	133,270	0	0	133,270	0
Lutein Ester	3,360	0	0	3,360	0
FAME	0	0	0	150,094	0
H_2SO_4	0	5,782	0	5,782	0

4.6.2 Methanol Recovery Distillation Column (T-301)

The inlet stream into the distillation column contains triglycerides, FAME, water, sulfuric acid, methanol, and chloroform. The distillate recovers 253,000 kg/day of methanol and 792 kg/day of chloroform. This is recycled back into acid esterification with a 25,500 kg/day purge

stream to prevent the accumulation of chloroform. The bottoms product contains 133,000 kg/day of triglycerides, 150,000 kg/day of FAME, 5,800 kg/day of sulfuric acid, 500 kg/day of methanol, and 8,800 kg/day of water. This is sent to the decanter for further separation. The distillation column contains 18 stages and is 1.9 m in diameter. The column height is 9.75 m. The feed enters above tray 12 and each stage is 0.61 m apart. The condenser heat duty is -6,193 kW and the reboiler heat duty is 6,343 kW.

4.6.3 Acid-Separation Decanter (V-302)

From the distillation column, the FAME and remaining triglycerides must be separated from the water and sulfuric acid. This separation was accomplished using the Olive Oil X9 decanter centrifuge manufactured by Alfa Laval. The bowl diameter is 0.575 m and the bowl length is 2.44 m. The bowl speed is 2900 rpm and the installed power is 45 kW. The overall machinery is 6 m long, 1.3 m wide, and 1.574 m tall. 302,000 kg/day is introduced to the decanter. Two streams exit. The light liquid phase contains 150,000 kg/day of FAME, 133,000 kg/day of triglycerides, 500 kg/day of water, and 270 kg/day of methanol. This is sent to base transesterification. The heavy liquid phase contains 270 kg/day of methanol, 8,300 kg/day of water, and 5,800 kg/day of sulfuric acid. This is considered an acid waste stream.

4.6.4 Acid Neutralization (M-301)

4,000 kg/day of NaOH are utilized to treat the acid waste stream from the decanter and neutralize 5,800 kg/day of H_2SO_4. The inlet stream from the decanter additionally contains 270 kg/day of methanol and 8,300 kg/day of water. The reaction converts the NaOH and H_2SO_4 into a total of 10,000 kg/day of water and 8,300 kg/day of Na_2SO_4. This process occurs in a mixing tank with a height of 0.5 m and a diameter of 0.4 m. The impeller diameter is 0.13 m and it

operates at 100 rpm. The stream is sent to municipal waste. Table 4.6-02 describes the material balances for methanol recovery and acid separation.

Table 4.6-02
Methanol Recover and Acid Separation Stream Table

Streams (kg/day)	**C5**	**C6**	**C7**	**C8**	**C9**	**C10**
Methanol	25,321	537	272	265	0	265
Chloroform	79	0	0	0	0	0
Water	110	8,781	499	8,282	0	10,406
FFA	0	0	0	0	0	0
Triglyceride	0	133,270	133,270	0	0	0
Lutein Ester	0	3,360	3,360	0	0	0
FAME	0	150,094	150,094	0	0	0
H_2SO_4	0	5,782	0	5,782	0	0
NaOH	0	0	0	0	4,012	0
Na_2SO_4	0	0	0	0	0	8,378

4.6.5 Base Transesterification and Saponification (R-302)

Base transesterification occurs at 65˚C with a reaction time of 20 minutes. 495,000 kg/day enter the CSTR. 204,000 kg/day of methanol are used in this reaction, recycled from a subsequent distillation column. 94,000 kg/day of FAME are produced, achieving a total of 244,000 kg FAME/day between esterification and transesterification. 10,000 kg/day of glycerol are generated from the transesterification reaction. Saponification leads to the production of 1,800 kg/day of free lutein and 82,000 kg/day of soap. The dimensions of the CSTR include a

tank height of 3.5 m and diameter of 2.2 m. The impeller diameter is 0.72 m and it operates at 81 rpm. The material balance is shown in Table 4.6-03.

Table 4.6-03
Base Transesterification and Saponification Stream Table

Streams (kg/day)	**C11**	**C12**	**C13**	**C22**
Methanol	0	200,192	225,513	203,479
Chloroform	0	0	79	132
Water	0	499	609	116
Triglyceride	0	39,388	39,388	0
Lutein Ester	0	0	0	0
FAME	0	243,976	243,976	0
KOH	3,653	3,653	3,653	0
Glycerol	0	10,234	10,234	0
Soap	0	23,051	23,051	0
Free Lutein	0	1,829	1,829	0

4.7 Solvent Separations and Recovery

The base esterification product stream is to be refined into a FAME-Lutein extract through solvent based separations starting with the phase separation and decantation of the organic chloroform phase containing both FAME and free lutein (V-303), followed by a solvent flash (H-301) to yield a mostly pure stream with both the products. To recover spent solvents from other esterification byproducts, a series of distillation columns (T-302 and T-303) were designed.

4.7.1 Chloroform/Methanol/Water Liquid-Liquid Extraction (V-303)

Given the necessity for a 10:10:9 Chloroform: Mixture:Water (by volume) stream, an additional 861,000 kg/day of chloroform and 522,000 kg/day of water is added to the incoming stream (which contains majority methanol). This provides a well separated set of 2 phases to be divided by decanting. The organic chloroform phase stream (C17) would have a total flow rate of 1,041,000 kg/day and would include 92% of the total lutein in the incoming stream (C13). The aqueous methanol stream (C15) would have the remaining lutein. The decanters used for this operation are identical to those found in the Lipid Extraction decanting section, the Alfa Laval X9 Olive Oil decanter with 3-phase separation modifications. These decanters use the same specifications outlined in section 4.5.3 and 4.6.3.

Table 4.7-01
CMW Liquid-Liquid Extraction Stream Table

Streams (kg/day)	**C13**	**C14**	**C15**	**C16**	**C17**
Methanol	225,513	0	214,171	0	11,342
Chloroform	79	861,037	66,964	0	794,153
Water	609	0	521,461	521,913	1,061
Triglyceride	39,388	0	32,691	0	6,697
FAME	243,976	0	18,972	0	225,004
KOH	3,653	0	3,032	0	624
Glycerol	10,234	0	8,933	0	1,301
Soap	23,051	0	23,051	0	0
Lutein	1,829	0	142	0	1,687

4.7.2 Solvent Flash and Recovery (H-301)

The solvent flash drum after the first liquid-liquid extraction operates at 135°C and 0.1 bar. The vessel is made of stainless steel and has a diameter of 3.2 m and a height of 3.66 m for a total volume of about 30 m^3. The heat duty provided by the heating coils is 3.88 MW and the electricity required by a compressor to pull 0.1 bar of vacuum is 62 kW. The total inlet and outlet flow rates are depicted in Table 4.7-0.

Table 4.7-02
Solvent Evaporator Stream Table

Streams (kg/day)	**C17**	**C18**	**C19**
Chloroform	794,153	792,905	1,248
Methanol	11,342	11,342	0
Water	1,061	1,061	0
Unreacted triglycerides	6,697	0	6,697
Glycerol	1,301	245	1,056
FAME	225,004	7,828	217,176
KOH	624	0	624
Lutein	1,687	0	1,687

4.7.3 Distillation to Remove Water, Glycerol, and Soap (T-302)

The light stream out of V-303 is fed to a distillation column at 802596 kg/day. The column is 17.1 meters tall with 30 stages and a diameter of 2.9 meters. The feed is positioned above stage 10, and the reflux ratio is set to 4 with a mole basis. The heat duties for the reboiler and condenser are 17,400 kW and 14,700 kW, respectively. The distillate consists of 214,171

kg/day methanol, 66,964 kg/day chloroform, and 116 kg/day of water and must be further separated. The bottoms product, stream C20, is then sent to be treated as hazardous waste.

Table 4.7-03
Distillation (T-302) Stream Table

Streams (kg/day)	**C15**	**C20**	**C21**
Methanol	214,171	116	214,055
Chloroform	66,964	0	66,964
Water	521,461	521,345	116
Triglyceride	32,691	32,691	0
FAME	18,972	18,972	0
KOH	3,032	3,032	0
Glycerol	8,933	8,933	0
Soap	23,051	23,051	0
Lutein	142	142	0

4.7.4 Distillation to Separate Chloroform from Recovered Methanol (T-303)

The distillate from the previous water methanol distillation column is sent to another distillation column to separate methanol and chloroform. The distillation column contains 20 stages. It has a diameter of 1.6 m and height of 10.97 m. The feed enters above stage 10. The reboiler heat duty is 3933 kW and the condenser heat duty is -3194 kW. 204,000 kg/day of methanol are recycled into base transesterification.

Table 4.7-04
Distillation (T-303) Stream Table

Streams (kg/day)	C21	C22	C23
Methanol	214,055	203,479	10,576
Chloroform	66,964	132	66,832
Water	116	116	0

4.8 Product Separation and Purification

The FAME and Lutein final product are separated from each other and refined via solvent extraction in the hexane/ethanol liquid-liquid extraction (V-401), Lutein antisolvent crystallization (M-401, V-403), and a final distillation column (T-401). Figure 4.8-01 gives an overview of the final product refinement steps in Process Section 4.

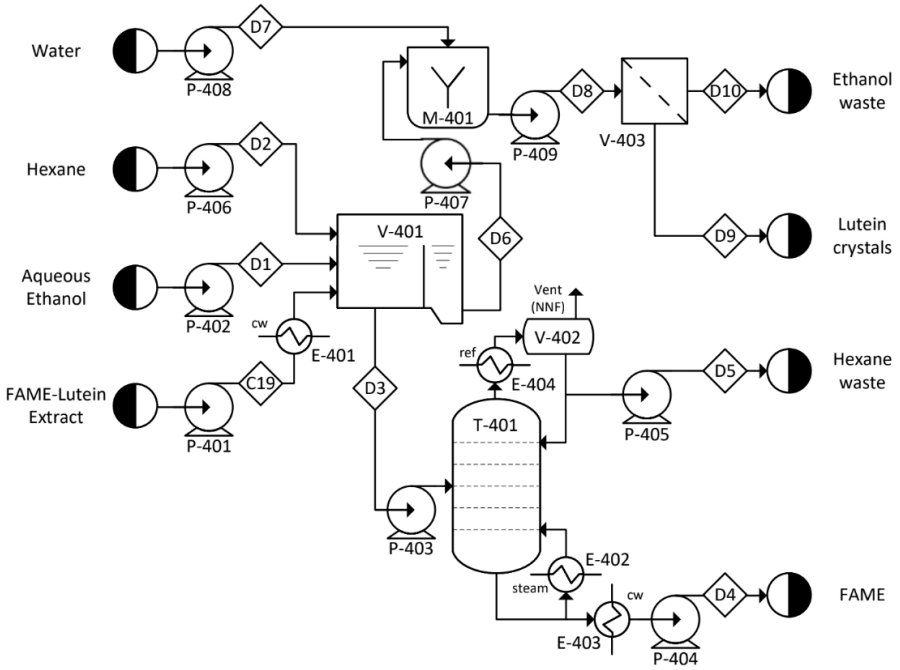

Figure 4.8-01: Process Section 4 - Product separation and purification

4.8.1 Hexane/Ethanol/Water Liquid-Liquid Extraction (V-401)

The final liquid-liquid extraction, using hexane and aqueous ethanol, uses the same equipment used in all of the other decanting operations throughout the process. An identical set 2 of Alfa Laval's X9 Olive Oil decanters are operated using the tricanter modification to separate the inlet streams (C19, D1, and D2) into the hexane-FAME extract stream (D3) and the aqueous ethanol with lutein extract (D6). These decanters would have a vessel for the incoming stream that is 0.575 m in diameter and 2.440 meters in length. The bowl would be operating at a maximum rotational speed of 2990 rpm with an electricity consumption of 45kW due to the power pack (Alfa Laval Inc., n.d.). Given this, a total of 83,600 kg/day of hexane and 58,300 kg/day of ethanol is added to the incoming FAME-lutein extract stream (C19) with an additional 45,826 kg/day of water also present in the ethanol feed stream. As a result, 1,650 kg/day would be separated into stream D6 and 205,464 kg/day of FAME would be separated into stream D3.

Table 4.8-01
HEW Liquid-Liquid Extraction Stream Table

Streams (kg/day)	**C19**	**D1**	**D2**	**D3**	**D6**
Chloroform	1,248	0	0	720	528
Hexane	0	0	83,645	83,064	581
Ethanol	0	58,344	0	2,976	55,368
Water	0	45,826	0	2,074	43,752
Unreacted triglycerides	6,697	0	0	264	15
Glycerol	1,056	0	0	70	986
FAME	217,176	0	0	205,464	11,712
KOH	624	0	0	0	624
Lutein	1,687	0	0	33	1,654

4.8.2 Lutein Crystallization and Filtration (M-401 and V-403)

The lutein crystallizer tank (M-401) is a 316SS 7500 L vessel with a 2.12 m height and diameter. The volumetric flow into the tank is 12,219 kg/hr. Assuming a specific gravity equivalent to water and a required residence time of 30 minutes, the working volume and flow rate exiting the tank is 6110L and 3.4 L/s respectively. The crystallizer is equipped with a 4-blade axial impeller made from 316SS with a polished finish. The impeller has a diameter of 28 inches and a speed of 80 rpm. The required power to drive the impeller is 2600W.

The lutein filtration system (V-403) consists of two cylindrical cross-flow polyvinylidene fluoride (PVDF) membranes. The two elements are configured such that one element is actively filtering the lutein slurry stream while the other is being regenerated to release lutein crystals. The filter elements are designed based on the V0.1-1-7940HF filter model from Synder Filtration systems. This microfiltration membrane filters out solids larger than 0.1 μm and has dimensions of 7.9” in diameter and 40” in length (Synder Filtration, n.d.). The volumetric flow into the filter is 12.9 m^3/hr resulting in a cross-membrane velocity of 0.55 cm/s. The resulting component mass flow rates for the lutein recovery process is shown in Table 4.8-02.

Table 4.8-02
Lutein Crystallization and Filtration Stream Table

Streams (kg/day)	**D6**	**D7**	**D8**	**D9**	**D10**
Chloroform	528	0	528	0	528
Hexane	581	0	581	0	581
Ethanol	55,368	0	55,368	0	55,368
Water	43,752	177,720	221,472	0	221,472
Unreacted triglycerides	360	0	360	0	360
Glycerol	986	0	986	0	986
FAME	11,712	0	11,712	0	11,712
KOH	624	0	624	0	624
Lutein	1,654	0	1,654	1,639	0

4.8.3 FAME-Hexane Distillation Column (T-401)

The hexane phase stream from V-401 is sent to a 30 stage distillation column and fed above stage 7. The column is 17.1 meters tall and 2.9 meters wide. The reflux ratio was set to 2 on a mole basis with a distillate rate of 4,000 kg/hr. The heat duty for the condenser is 2300 kW. The reboiler must utilize natural gas as the solution is heated to 294ºC with an associated heat duty of 3900 kW. The bottoms product consists of pure FAME (D4) which is then cooled using a heat exchanger (E-403) with a heat duty of -1590 kW. The distillate consisting primarily of hexane at 3460 kg/hr is discarded as hazardous waste.

Table 4.8-03
FAME-Hexane Distillation Stream Table

Streams (kg/day)	**D3**	**D4**	**D5**
Chloroform	720	0	720
Methanol	0	0	0
Water	2074	0	2074
Unreacted triglycerides	6336	0	6336
Glycerol	70	0	70
FAME	205262	204634	830
KOH	0	0	0
Lutein	33	0	33
Hexane	3461	0	3461

5. Economic Considerations

5.1 Total Capital Costs

The following subsections detail plant capital cost as they pertain to key unit operations and ancillary pumps and heat exchangers.

5.1.1 Algae Cultivation

The main equipment involved in this process is related to the cultivation and harvesting of the algae. This includes an inlet tank to hold swine waste and supplemental water, raceways with pond liners and paddlewheels, dissolved air flocculation units, bead mills, and a conveyor belt dryer system with a heater. The initial cost of the stainless steel inlet mixing tank was estimated using Capcost. The cost of the raceways was first estimated using the average costs to install a pond which averaged $4 per cubic meter of space (HomeGuide, 2024). The raceways then all require a PVC liner costing $1.18 per square foot ("Agtec 45mil RPP Pond and Chemical Containment Geomembrane Liner (Custom Size)", 2024). The paddle wheels to drive flow must each be custom-made with the cost per foot in diameter estimated by Water Wheel Factory at $1290 (Waterwheel Factory, 2024). 216 extra paddle wheels were accounted for to provide enough spares to cover one batch of algae. The E-1035 DAF model was used from Ecologix, and five units are needed. The DYNO-MILL ECM-AP 60 from WAB Group was used as the bead mill and 200 units are needed. 2,161 conveyor belt dryers are utilized to reduce the water content of the algae. The cost of the dryers was scaled up from the model designed by Hosseinizand et al. (2018) and adjusted by the CEPCI to reflect current prices. 2,161 blowers are needed to generate airflow within the dryers. The cost of the dryer heater and the dryer blowers was found in cost graphs from Peters et al. (2003). The capital costs are shown in Table 5-01.

Table 5.1-01
Algae Cultivation Equipment Capital Costs

Equipment	Size	Material	Quantity	Total Price (USD)
M-101	Diameter: 8.5 m Height: 8.5 m	Stainless Steel	1	1,870,000
R-101	Length: 34.5 m Width: 5.8m Depth: 2.2m	Compact Gravel and PVC Liner	4321	29,890,000
Paddle Wheels	Diameter: 4.27 m Width: 2.9 m	Stainless Steel	4537*	81,938,220
V-101,102	Length: 13.2 m Width: 3.4 m Height: 3.3 m	Stainless Steel	5	3,400,000
E-101	Power: 86,000 kW	Carbon Steel	1	202,224
Blowers	Capacity: 0.82 m^3/s	Stainless Steel	2,161	10,926,016
H-101	Length: 39 m Width: 3 m Material Depth: 0.5 m	Belt	2,161	421,296,295

*More paddlewheels than raceways to have spares

5.1.2 Crude Lipid Extraction

The equipment for the crude lipid extraction process includes mixing tanks and impellers, disk stack centrifuges, decanters, a distillation column, and a flash drum. There are 15 mixing tanks with 15 impellers made of stainless steel, priced using a quote from Portland Kettle Works. The price of the 25 disk stack centrifuges was found using Capcost. The cost for the 284 decanters was found on IndiaMART. The distillation column was modeled in Aspen and the cost includes that of the tower, condenser, reboiler, and reflux pump. Therefore these costs will be

omitted in discussions of ancillary equipment prices. Aspen Plus was also used to model and determine the cost of the flash drum. The capital costs are shown in Table 5-02.

Table 5.1-02
Crude Lipid Extraction Equipment Capital Costs

Equipment	Size	Material	Quantity	Installed Price (USD)
R-201 (vessel) R-201 (impeller)	Diameter: 2.7 m Height: 4.7 m Diameter: 0.84 RPM: 300	Stainless Steel	15	2,250,000
R-202	Outer Diameter: 0.3 m Flow Rate: 25 L/s RPM: 3740	Stainless Steel	25	2,950,000
V-201	Diameter: 1.3 m Height: 1.574 m Volume per Unit: 0.63 m^3	Stainless Steel	284*	512,904
T-201	Diameter: 4.3 m Height: 17.1 m	Stainless Steel	20	67,880,000
H-201	Diameter: 14.9 m Height: 3.66 m Volume: 641 m^3	Stainless Steel	1	2,079,300

*Number of decanters is so large due to the enormous flow rate requirements

5.1.3 Acid Esterification and Base Transesterification

The equipment for the acid esterification process includes three CSTRs made of stainless steel and three impellers. The acid separation and neutralization steps require a distillation column, a decanter, and a mixing tank and impeller. The distillation column was modeled in Aspen and the cost includes that of the tower, condenser, reboiler, and reflux pump. Therefore these costs will be omitted in discussions of ancillary equipment prices. The price of the decanter was found on IndiaMART. The base transesterification utilizes one CSTR and one impeller. For

all CSTRs and the mixing tank, the price was determined using Capcost. The impellers are four blade axial turbines and the cost was found on INDCO. The costs are shown in Table 5.1-03.

Table 5.1-03
Acid Esterification and Base Transesterification Equipment Capital Costs

Equipment	Size	Material	Quantity	Installed Price (USD)
R-301 (vessel)	Diameter: 2.6 m Height: 3 m Volume per Unit: 13.9 m^3	Stainless Steel	3	744,000
R-301 (impeller)	Diameter: 0.87 m RPM: 48			8,364
T-301 (condenser)	Heat Transfer Area: 216.49 m^2 Heat Duty: -6170 kW	Stainless Steel	1	1,006,700
T-301 (tower)	Diameter: 1.9 m Height: 9.75 m Volume: 27.6 m^3			
T-301 (reboiler)	Heat Transfer Area: 174 m^2 Heat Duty: 6684 kW			
V-302	Diameter: 1.3 m Height: 1.574 m Volume per Unit: 12.3 m^3	Stainless Steel	1	1,806
M-301 (vessel)	Diameter: 0.4 m Height: 0.5 m Volume per Unit: 0.57 m^3	Stainless Steel	1	71,600
M-301 (impeller)	Diameter: 0.13 m RPM: 100			594
R-302 (vessel)	Diameter: 2.2 m Height: 3.5 m Volume per Unit: 8 m^3	Stainless Steel	1	219,000
R-302 (impeller)	Diameter: 0.72 m RPM: 81			2,030

5.1.4 Solvent Separations and Product Purification

The chloroform/methanol/water liquid-liquid extraction outlined in sections 3.10.1 and 4.7.1 uses 8 Alfa Laval X9 decanters for the 1,680,000 L/day processed in the operation. Cost of these decanters are featured in table 5.1-04 under V-303. Recycling the methanol stream from the CMW liquid-liquid extraction requires two distillation columns (T-302 and T-303) which were both modeled in Aspen resulting in an inclusive cost of the tower, reboiler, condenser, and reflux pump. As with the CMW LLE, the hexane/ethanol/water LLE uses the same decanters found in V-303 on table 5-03 however for the 20,603 L/day processed by this operation, only 3 such decanters are necessary. The column to separate out the FAME (T-401) was modeled in Aspen with an inclusive cost of the tower, reboiler, condenser, and reflux pump.

Table 5.1-04
Solvent Separations and Product Purification Equipment Capital Costs

Equipment	Size	Material	Quantity	Installed Price (USD)
V-303	Diameter: 1.3 m Height: 1.574 m Volume per Unit: 12.3 m^3	Stainless Steel	8	14,448
T-302	Diameter: 2.9 m Height: 17.1 m	Stainless Steel	1	2,116,000
T-303	Diameter: 10.97 m Height: 1.6 m	Stainless Steel	1	1,091,500
H-301	Diameter: 3.2 m Height: 3.66 m Volume: 29.4 m^2	Stainless Steel	1	337,300
V-401	Diameter: 1.3 m Height: 1.574 m Volume per Unit: 12.3 m^3	Stainless Steel	3	5,418
T-401	Diameter: 2.9 m Height: 17.1 m	Stainless Steel	1	1,663,000
M-401 (vessel) M-401 (impeller)	Diameter: 2.122 m Height: 2.122 m Diameter: 0.71 m	Stainless Steel	1	60,830
V-403	Diameter: 0.20 m Length: 1.02 m	Stainless Steel, PVDF	2	488,000

5.1.5 Ancillary Equipment

The two types of ancillary equipment that were considered in the plant design were pumps and heat exchangers. Pump capital costs were calculated using the West Virginia University's 2017 Capcost spreadsheet. To do this, power requirements for each pump (P) in Watts were calculated using the equation below where "p" is differential pressure in Pascals and "Q" is volumetric flow rate in m^3/s.

$$P = p * Q \tag{5-01}$$

The differential pressure for each pump was estimated by summing the actual pressure difference between the units the pump was located between, additional pressure due to frictional losses, and gravity head. If the pressure difference was negative (for example transporting to vessels operating at lower pressures), it was subtracted from the pressure due to frictional losses and the gravity head. Further assumptions were made when calculating pressure losses due to friction and are as follows: 0.5 atm were allotted for piping, 0.5 atm were allotted for every heat exchanger, and 0.5 atm were allotted for every control valve. Every pump was considered to have a control valve and any point where a line split occurred was also considered to have a control valve on each branch of the split. Pressure due to gravity head (p) in Pascals was calculated according to equation 5-02 where the fluid density (ρ) in kg/m^3 was averaged based on the composition of the fluid, "g" is the acceleration due to gravity in m/s^2, and "h" is the vertical height in meters the fluid had to travel to enter a tall vessel.

$$p = \rho * g * h \tag{5-02}$$

The type of pump was determined by Capcost based on the power requirement. For all pumps that require less than 1 kW, calculated from equation 5-01, Capcost could only return a

price for reciprocating pumps. For any pumps that required more than 1 kW, a centrifugal pump was used.

The material of construction for each pump was determined from chemical compatibilities. For all pumps transporting very dilute mixtures (all streams before addition of solvents in lipid extraction and one water recycle stream), carbon steel was used as it is the standard in the water industry. For all of the pumps transporting slightly corrosive solvents such as chloroform, methanol, salts, etc., stainless steel was used to prevent their degradation. For all of the streams with any amount of sulfuric acid however, specialized polypropylene pumps were quoted from chemical pump suppliers: Ryan Herco Flow Solutions or Magdrivepump.com. This is due to the extremely corrosive nature of sulfuric acid. Capcost does not contain polypropylene as a pump material and was therefore not used in the cost estimation of these pumps.

In addition, spare pumps were factored into the overall capital cost. For unique pumps with a single pump in operation, only one spare was accounted for. However, for non-unique pumps with multiple units in operation, about one fourth of the total pumps in operation were added as spares to have inventoried. Table 5.1-05 outlines the capital costs associated with all of the pumps based on their type, construction material, hydraulic power, and quantity.

Table 5.1-05
Pump Capital Costs

Equipment	Type	Hydraulic Power (kW)	Quantity (spares)	Total Purchased Cost (USD)
P-101	Carbon steel centrifugal	16	1 (1)	29,800
P-102	Carbon steel centrifugal	98	1 (1)	79,700
P-103	Carbon steel centrifugal	16	5 (2)	105,000
P-104	Carbon steel centrifugal	4	5 (2)	67,300
P-105	Carbon steel centrifugal	6	20 (5)	262,000
P-201	Stainless steel centrifugal	24	1 (1)	52,600
P-202	Stainless steel centrifugal	54	1 (1)	80,700
P-203	Stainless steel centrifugal	53	1 (1)	79,900
P-204	Stainless steel centrifugal	137	1 (1)	148,000
P-205	Stainless steel centrifugal	53	1 (1)	79,800
P-301	Stainless steel reciprocating	0.7197	1 (1)	63,600
P-302	Polypropylene mag-drive	0.0038	1 (1)	345
P-303	Stainless steel reciprocating	0.0971	1 (1)	44,900
P-304	Polypropylene mag-drive	1.18	1 (1)	20,316
P-305	Polypropylene mag-drive	0.5830	1 (1)	20,316
P-306	Stainless steel reciprocating	0.9409	1 (1)	68,800
P-307	Stainless steel reciprocating	0.3748	1 (1)	54,100
P-308	Polypropylene mag-drive	0.0139	1 (1)	345
P-309	Polypropylene mag-drive	0.0224	1 (1)	345
P-310	Stainless steel reciprocating	0.3009	1 (1)	51,800
P-311	Stainless steel centrifugal	1.42	1 (1)	23,100
P-312	Carbon steel centrifugal	22	1 (1)	33,500
P-313	Stainless steel centrifugal	24	1 (1)	52,900
P-314	Stainless steel centrifugal	1.06	1 (1)	22,600
P-315	Stainless steel reciprocating	0.6893	1 (1)	62,800
P-317	Stainless steel reciprocating	0.3694	1 (1)	54,000
P-401	Stainless steel reciprocating	0.0697	1 (1)	44,900
P-402	Stainless steel reciprocating	0.5921	1 (1)	60,500
P-403	Stainless steel reciprocating	0.2105	1 (1)	48,700
P-404	Stainless steel reciprocating	0.2343	1 (1)	49,400
P-405	Stainless steel reciprocating	0.4000	1 (1)	54,900
P-406	Stainless steel reciprocating	0.1535	1 (1)	46,600
P-407	Stainless steel reciprocating	0.1474	1 (1)	46,200
P-408	Stainless steel reciprocating	0.1535	1 (1)	46,700
P-409	Stainless steel reciprocating	0.2084	1 (1)	48,700
Total			64 (41)	2,070,466

The price of heat exchangers was determined using Aspen Plus. Heat exchangers were modeled as heater blocks and the utility was set to steam or cooling water. The capital cost of reboilers and condensers of distillation columns are not included in this table and are found in the capital cost of the distillation column itself. The costs are summarized in Table 5-06. Note, the costs for the heat exchangers for H-201 and H-301 are separate from the previously listed equipment costs due to the fact that the flashes were modeled in two steps: first by heating the process stream to the desired temperature with a heat exchanger and then second with a flash at low pressure. Thus, the costs listed below are only for the heat exchangers present in the process.

Table 5.1-06
Heat Exchanger Capital Costs

Equipment	**Heat Duty (kW)**	**Heat Transfer Area (m^2)**	**Installed Cost (USD)**
E-202	-36794	4714	1,624,100
E-204	-76174	2607	909,100
E-301	-390	8.7	85,000
E-302	-49	1.9	78,600
E-305	-428	9.1	85,000
E-306	-661	52.4	120,400
E-307	-3187	57.8	126,000
E-309	-2000	73	129,600
E-401	-651	13	85,400
E-403	-1597	36.7	108,100
H-201	76776	3175	1,140,700
H-301	3885	52.8	133,100
Total estimated cost			4,625,000

5.1.6 Total Capital Cost

The total plant capital cost was calculated according to Peters et al. (2003). This method consists of using the total equipment purchase price and multiplying by different factors to estimate: direct costs including purchased-equipment installation, instrumentation and controls, piping, electrical systems, buildings, and more; indirect costs including engineering and supervision, construction expenses, legal expenses, etc.; and working capital. The sum of the direct costs and indirect costs was calculated by multiplying the total purchased equipment cost by a factor of 4.28 (Peters et al., 2003). In addition to these expenses, land costs were calculated based on the average price of land in Duplin County, NC according to listings on Landsearch.com. The algae raceways require 214 acres of land not including walkways between each raceway. Therefore, a conservative estimate of about 320 acres for the entire plant, including all of the processing steps was assumed and at an average cost of $10,884/acre, the cost of land totals to about $3.5 million. Adding the land cost to the sum of the direct and indirect costs is the fixed capital investment. The working capital was calculated by multiplying the purchased equipment cost by 0.75. The sum of the fixed capital investment and the working capital is the total plant capital cost. These capital costs are summarized in Table 5.1-07. Note, the total equipment purchase costs were adjusted for each section because the costs taken from Aspen Plus V14 models included installation costs, however, installation is accounted for already in the correlation provided by Peter et al. (2003).

Table 5.1-07
Total Capital Costs

Expenses	Estimated Price (USD)
Algae Cultivation	536,800,000
Crude Lipid Extraction	56,000,000
Acid Esterification and Base Transesterification	1,700,000
LLE and Product Purification	4,200,000
Ancillary Equipment	4,200,000
Total equipment purchase price	603,000,000
Direct and indirect costs	2,581,300,000
Land	3,500,000
Fixed capital investment	2,584,800,000
Working capital	450,000,000
Total plant capital cost	3,035,000,000

5.2 Yearly Operating Costs

The following subsections detail plant operating cost as they pertain to starting material, utilities, labor, waste management, and property insurance and taxes.

5.2.1 Raw Materials

In determining the price of the materials used in the operations, bulk prices were considered and shipping costs were not taken into consideration. Given this, the following numbers were gathered for each of the different materials.

Table 5.2-01
Make Up Materials Costs

Make Up Material	Yearly Amount (kg)	Price per Unit Mass ($/kg)	Yearly Cost ($/yr)	Citation
Swine Waste	1,321,943,276	0.020	26,438,865	(Ladmin, 2019)
Water	3,706,501,540	1.48E-5	54,856	
Chloroform	32,637,478	0.473	15,437,528	(*Chloroform prices: Historical and current* 2019)
Methanol	14,638,154	0.295	4,318,175	(*Methanol prices: Current and forecast* 2019)
H_2SO_4	1,931,188	0.055	106,408	(*Sulfuric acid prices: Historical and current* 2019)
KOH	1,220,102	0.840	1,024,885	(*Potassium hydroxide prices: Historical and current* 2019)
NaOH	1,373,408	0.26	357,086	(*Sodium hydroxide price index* 2023)
Hexane	27,937,363	1.352	37,771,315	(Manufacturers, 2023)
Ethanol	19,487,418	0.433	8,438,052	(*Ethanol price: Current and forecast* 2019)
Total estimated cost			94,000,000	

5.2.2 Utilities: Electricity

There are many sources of electricity usage among all of the aforementioned unit operations. When calculating the electricity usage of the pumps, the hydraulic power calculated from (5-01) was then divided by an efficiency of 0.7 as an estimate of overall pumping efficiency. The cost of industrial electricity in Duplin County, NC was assumed to be $0.0594/kWh according to Electricitylocal (n.d.). Cost per year was calculated on a 334 work

day schedule operating 24 hours a day. Table 5.2-02 summarizes all of the electricity usage and the yearly cost with regards to electricity.

Table 5.2-02
Electricity Utility Costs

Equipment	**Quantity**	**Total power requirement (kW)**	**Cost of electricity (USD)/year**
Paddlewheel motors	4321	203	96,700`
DAF Compressor	1	53	25,235
Bead mill feed tank impeller	20	10.52	5,009
Beadmills	200	26400	12,570,370
Centrifuge	2	2500	1,190,376
Acid Neutralization Impeller	1	0.001	0.48
Base Transesterification Impeller	1	2.6	1,234
Crystallizer tank impeller	1	2.6	1,238
LE Evap vacuum	1	52	24,912
LLE Evap vacuum	1	62	29,521
Pumps	64	519	352,960
Total estimated cost			14,200,000

5.2.3 Utilities: Steam, Cooling Water, and Natural Gas

Steam and cooling water are utilized in the heater for the dry air in the conveyor belt, in heat exchangers, and in the condenser and reboiler of distillation columns. The FAME distillation column reboiler operates at such a high temperature that steam cannot be used and a fired natural gas heater must be used. The heat exchangers were modeled as heater blocks in Aspen Plus. Utility costs for steam, cooling water, and natural gas were calculated using Aspen Plus. Cooling water was assumed to be at 17˚C, the yearly average dew point temperature of Duplin County, NC. Costs for steam, cooling water, and natural gas are shown in Table 5.2-03.

Table 5.2-03
Steam, Cooling Water, and Natural Gas Prices

Equipment	Utility	Total Cost per Year ($)
E-101	Low Pressure Steam	5,466,912
E-201	Cooling Water	35,959
E-202	Steam	44,128,080
E-204	Cooling Water	459,316
E-301	Cooling Water	2,389
E-302	Cooling Water	299
E-303	Cooling Water	56,690
E-304	Steam	1,674,703
E-305	Cooling Water	2,624
E-306	Cooling Water	4,049
E-307	Cooling Water	19,800
E-308	Steam	1,102,883
E-309	Cooling Water	12,264
E-310	Cooling Water	89,871
E-311	Steam	985,407
E-312	Cooling Water	35,959
E-401	Cooling Water	1,347
E-402	Natural Gas	475,108
E-403	Cooling Water	9,699
E-404	Cooling Water	232,985
H-201	Steam	4,199,582
H-301	Steam	246,492
R-102	Cooling water	94,909
Total estimated cost		59,340,000

5.2.4 Labor Costs

The number of operators required for this plant was determined using the following equation proposed by Turton (2018) shown in (5-03).

$$N_{OL} = \left(6.29 + 31.7P^2 + 0.23N_{NP}\right)^{0.5} \quad (5\text{-}03)$$

N_{OL} refers to the number of operators per shift. P is the number of particulate handling steps, and N_{NP} is the number of non-particulate handling steps. The number of particulate and non-particulate handling steps are summarized in Table 5.2-04. It was assumed that one non-particulate step would be assigned per group of 20 raceways, group of 20 bead mills, group of 20 dryers, and group of crude lipid extraction decanters. It was assumed that raceways, handling KOH, handling NaOH, and filtration would each count as one particulate handling step.

Table 5.2-04
Particulate and Non-Particulate Handling Steps

	Particulate Steps (P)	**Non-Particulate Steps (N_{NP})**
Algae Cultivation	1	336.1
Crude Lipid Extraction	0	57.2
Esterification	2	9
Separations	1	23
Heat Exchangers	0	11
Total	4	436.3

The equation yields 24.8 operators per shift. The number of operators per shift needs to be scaled by the number of shifts per year and the number of shifts per operator in order to determine the amount of operators required. The N_{OL} value is scaled by 4.5, giving a total

operator count of 112. The average salary for a Chemical Plant Operator I in North Carolina is $46,506 (“Chemical Plant Operator I Salary in North Carolina”, n.d.). The supervision costs were assumed to be an extra 15% and insurance and social security were assumed to be an extra 40% in addition to wages (Peters et al., 2003). Labor costs are shown in Table 5.2-05.

Table 5.2-05
Operating Labor Costs

	Cost per Year ($)	**Insurance ($)**	**Total Cost per Year ($)**
Operators	5,185,000	2,074,000	7,529,000
Supervisors	777,750	311,100	1,088,850
Total estimated cost			8,350,000

5.2.5 Waste Treatment Costs

Any streams containing chloroform, ethanol, hexane, and/or sulfur were marked for specialized waste treatment due to the inability for local water treatment to properly process said streams. In order to form an itemized list of streams and costs, a classification system from the Clean Harbors disposal code was used.

Table 5.2-06
Waste Stream Classification and Cost

Stream	Description	Clean Harbors Disposal Code	Flow Rate (gal/yr)	Rate ($/gal)	Cost ($/yr)
B4	Lysed Cells & Chloroform	FB4	41,514,864	4.31	178,981,900
C10	Sodium Sulfate	A40	1,225,590	5.03	6,164,498
C21	Water Glycerol Soap	-	-	-	-
D10	Ethanol Waste	FB1	280,104	2.06	577,321
D5	Hexane Waste	FB1	2,786	2.06	5,743
Total estimated cost					186,000,000

In addition to these costs, North Carolina has a 0.70 $/ton hazardous waste generation tax. Given the total flow rate of 176,757 tons/yr the tax costs a total of $ 125,130 per year (NC DEC, 2023).

5.2.6 Insurance and Property Taxes

The yearly insurance cost was estimated as 1% of the fixed capital investment (Peters and Timmerhaus, 1991). The property tax was determined from Small Business Property Tax Advisors who cite the property tax in Duplin County, NC to be $0.735 per $100 of assessed value (SBPTA, n.d.). Assessed value was equated to fixed capital investment in this case. Therefore, the insurance costs $25,800,000 per year and property tax costs $19,000,000 per year.

5.3 Revenues and Yearly Net Profit

In a year of production at full capacity, the revenue generated by FAME is approximately $94 million whereas the revenue generated by lutein is approximately $33 million. The revenue from FAME was based on the current market price of $4.6/gal of B100 (the specific grade of biodiesel being produced) according to Statista (n.d.). The revenue from lutein was based on the current market price of $60/kg according to Pharmacompass (n.d.). The yearly operating costs subtracted from the yearly revenues are depicted in Table 5.3-01. In short, there is a net loss of about $280 million per year. This is primarily due to a lack of recycling throughout the process causing waste treatment to be quite expensive. Trace chemicals such as chloroform contaminate many streams; purification would be required to reuse chemicals such as hexane, but this was deemed out of scope for this project.

Table 5.3-01
Yearly Net Loss

Revenues	**(USD/year)**
FAME	+94,400,000
Lutein	+33,100,000
Operating costs	**(USD/year)**
Raw materials	-94,000,000
Utilities	-73,500,000
Labor	-8,350,000
Waste treatment	-186,000,000
Insurance	-25,800,000
Property tax	-19,000,000
Net loss	-279,275,000

The lack of profitability on a year to year basis alone causes this operation to be impossible without heavy government subsidies on B100. Therefore, the operation in its current state is not a sound investment and will lead to significant financial losses.

5.4 Scenario Based Discounted Cash Flow Analysis

The following is a theoretical economic analysis to illustrate possible avenues of creating a return on investment and an internal rate of return that may change the previous recommendation to turn this project down.

5.4.1 DCF Scenario 1

First, a scenario in which the market prices of B100 and free lutein rise from $4.6/gal and $60/kg to $15/gal and $200/kg respectively. These prices were chosen to achieve minimal yearly profits for the sake of economic analysis. With these market prices, the gross profit per year is approximately $10.5 million, a nominal amount compared to the initial capital cost.

Next, an internal rate of return (IRR) was calculated by achieving a neutral net present value (NPV) from the discounted cash flow (DCF) at the end of the plant's lifespan. The DCF was calculated from the product of discount factors dependent on the IRR and actual cash flow values (ACF) for every year of the plant's construction and operation. The actual cash flow was calculated over 20 years under the assumption that the typical lifespan of a chemical processing plant is 20 years. However, it was assumed that the construction of the plant would occur over a period of 18 months and that all of the capital cost would be spent evenly over this time period. Therefore, during year -1, the actual cash flow is two thirds of the total capital cost. For the remaining 6 months of year 0, after the last third of the total capital cost is spent, it was assumed that the plant would operate at half capacity (thus only producing a quarter of normal yearly revenue at half of the normal yearly operating cost) due to start-up difficulties that would need to be resolved. After year 0, the plant was assumed to operate at full capacity for 20 years. In addition, the North Carolina corporate income tax of 2.5% and the federal corporate income tax of 21% were combined and applied to a 10 year straight-line depreciation schedule followed by another 10 years of no tax breaks to create a 20 year actual cash flow table. For this scenario, an IRR of about -14% was calculated after 20 years, which means the initial capital cost was never regained in profits. A summary of the gross profit and actual cash flow table is portrayed in Table 5.4-01 and Table 5.4-02 respectively.

Table 5.4-01
Scenario 1 Gross profit

Revenues	**(USD/year)**
FAME	+307,800,000
Lutein	+109,500,000
Operating costs	-406,775,000
Gross profit	+10,525,000

Table 5.4-02
Scenario 1 Actual Cash Flow (ACF)

Year	**ACF (USD)**
-1	-2,026,666,667
0	-705,370,833
1 : 10	+79,491,625
11 : 20	+8,051,625
Total	-1,856,600,000

Since IRR is computed based on achieving a neutral sum of the discounted cash flow. A graph of the DCF is provided below in Figure 5.4-01. The resulting IRR was -14%. The discount rate was numerically determined for each year by setting the discount factor for year 0 to 1 and adding the IRR to 1 for year -1 and then subtracting the IRR from 1 and multiplying by the

previous year's discount factor. For this reason, due to the nature of the IRR being negative, the discount factor from year to year continuously increased in order to achieve an NPV of 0.

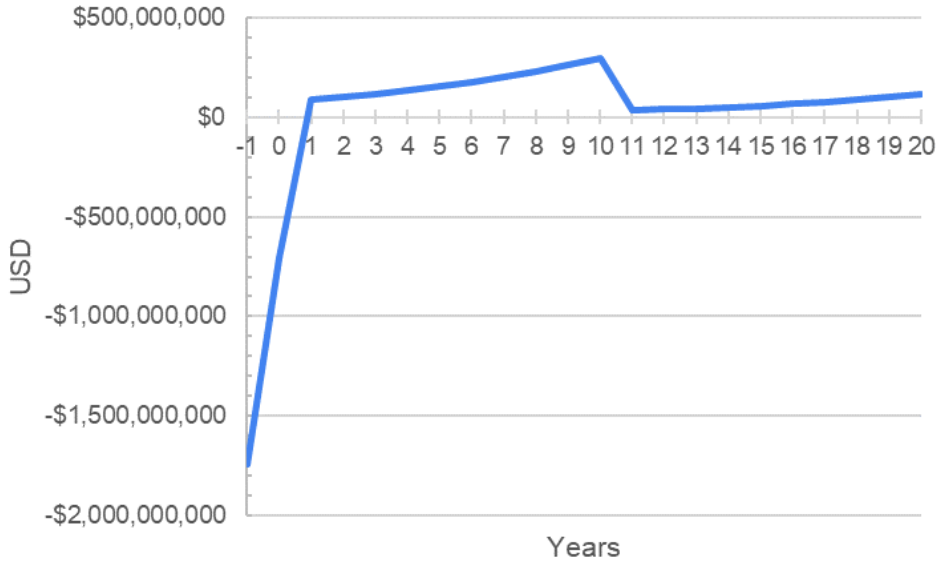

Figure 5.4-01: Scenario 1 DCF over plant lifespan

As evidenced by Figure 5.4-01, even with minimal profits after theoretical market price raises, the initial capital investment cannot be overcome. Therefore, a second scenario that reduced initial capital investment and decreased operating costs was analyzed.

5.4.2 DCF Scenario 2

In scenario 2, the initial capital investment was reduced considerably by reducing the purchase price of the industrial dryers used prior to lipid extraction from about $420 million to $100 million. This reduced the overall capital cost, after scaling, to about $1.4 billion instead of over $3 billion. In the event that advancements in technology with regards to the dewatering of microalgae occur, this reduction in scale and purchase price may very well be reasonable and would greatly affect the profitability of a process such as this one. In addition to reducing the initial capital cost, the operating cost for waste treatment was reduced from $186 million to $20

million with the justification that a chemical processing plant such as this would have their own waste treatment plant that would cost significantly less than paying to treat hazardous waste. As the design of a waste treatment plant was outside the scope of this design project, this DCF scenario may more accurately reflect the overall operating cost of the plant. In this scenario, the market prices of FAME and lutein were also still inflated to $15/gal and $60/kg for the sake of comparison to scenario 1. The gross profit and actual cash flow for this scenario are shown in Tables 5.4-03 and 5.4-04 respectively.

Table 5.4-03
Scenario 2 Gross profit

Revenues	**(USD/year)**
FAME	+307,800,000
Lutein	+109,500,000
Operating costs	-216,965,000
Gross profit	+200,335,000

Table 5.4-04
Scenario 2 Actual Cash Flow (ACF)

Year	ACF (USD)
-1	-946,666,667
0	-260,275,833
1 : 10	+186,626,275
11 : 20	+153,256,275
Total	2,191,900,000

As shown by the actual cash flow final sum, a profit is made and the initial capital cost is overcome in this scenario. Figure 5.4-02 below shows the DCF for scenario 2 over the lifespan of the plant. The DCF was computed the same way as scenario 1, however due to the positive nature of the IRR, the discount rate leveled off over the plant lifetime as an NPV of 0 was still achieved.

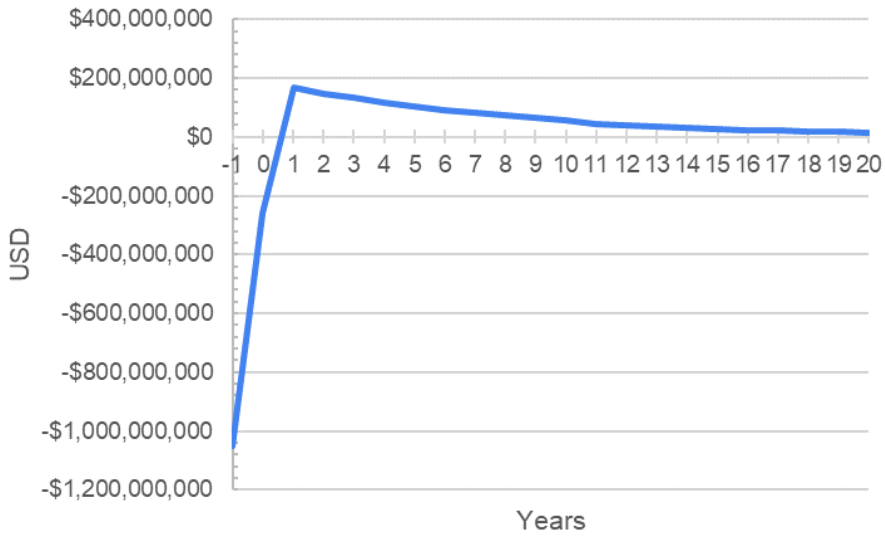

Figure 5.4-02: Scenario 2 DCF over plant lifespan

In this scenario, the DCF behaves as one would expect, decreasing continuously over the lifespan of the plant as losses are recouped instead of rising towards the end of the depreciation period and end of the plant lifespan to achieve a neutral net present value. Overall, the computed IRR of this scenario is about 11%.

5.4.3 DCF Conclusions

In conclusion, as the project stands as it is designed and selling FAME and lutein at current market prices, this project is not financially feasible because the operating cost outweighs the revenues. However, at inflated market prices slight yearly profits can be made but over a 20 year plant lifespan, the initial capital cost will not be recouped and the project will still result in overall financial loss. Finally, a profit can be achieved if technological advancements are made to the dewatering process, thus reducing dryer prices to a quarter of their original price and there is a built-in waste treatment plant in addition to inflated market prices. However, despite making a profit in this scenario, the IRR is only 11%. Due to the high risk nature of this type of project

(due to the fact that biodiesel production from algae is not a proven profitable process), the threshold rate was chosen to be 30-40% in order to solicit a recommendation to follow through with the project. Since the computed IRR of 11% falls well below the threshold rate, even with this profitable scenario, this project should remain out of consideration for investors due to the high-risk nature of the endeavor.

6. Safety and Environmental Considerations

6.1 Health and Safety Considerations

The making of lutein and FAME outlined in this report makes use of chemicals and processes that have harmful characteristics, which may hurt individuals that are near or come in contact with them. Additionally, copious quantities of hazardous chemicals are used and immediately discarded, creating excessive hazardous waste. Given this, a summary of the safety considerations of chemicals (both individually and in mixtures) employed in this process will be presented.

6.1.1 Chemical Hazards

Table 6.1-01
Overview of Chemical Hazards

Chemical Name	**NFPA Diamond**	**Intrinsic/Notable Hazards**
Chloroform		Acute Toxic Health Hazard
Ethanol		Highly Flammable
FAME		Health Hazard
Glycerol		N/A Environmental Hazard
Hexane		Highly Flammable Irritant Health Hazard Environmental Hazard
Lutein		N/A
Methanol		Highly Flammable Acute Toxic Health Hazard
Potassium Hydroxide		Corrosive Irritant
Sodium Hydroxide		Corrosive
Sulfuric Acid		Corrosive

Although the manner in which dangerous chemicals can be released inadvertently are too numerous to consider within the constraints of this report, an example case of the largest possible release in the plant is explored. Stream B7, the inlet stream to the large methanol-water distillation column, contains large amounts of methanol. The stream carries 23,286,336 kg/day of methanol alongside 22,569,456 kg/day of chloroform. Through a possible pump seal failure at pump P-204 these two chemicals might leak out. While both of these chemicals are acutely toxic towards workers in the area (with chloroform being much more toxic), the primary concern upon a methanol release is the ignition of the subsequent methanol cloud. Thus, the mapped dispersion of methanol and chloroform are flammability and toxicity respectively. The conditions used are 22°C at high humidity with average cloud coverage. Wind speeds of 14 km/h were used.

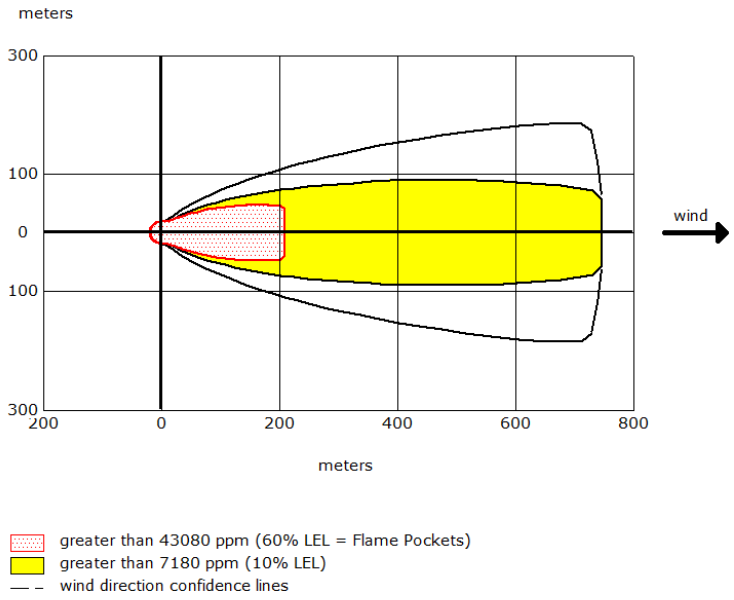

Figure 6.1-01: Methanol flame dispersion

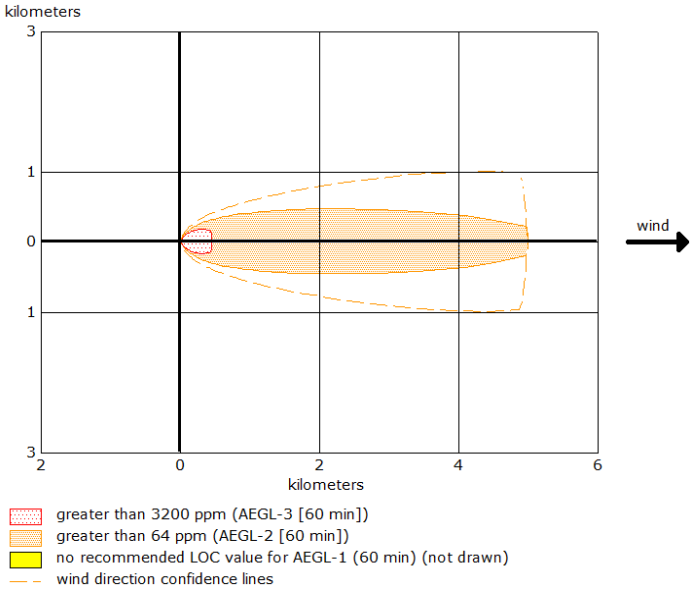

Figure 6.1-02: Chloroform toxic vapor dispersion

This particular case explores both methanol and chloroform releases in large quantities. Such conditions under which both these chemicals are found in similar amounts are quite common throughout the operation seen in streams B3 through B8 excluding B4. Additional cases in which one of two chemicals is found in significant quantities are also present.

To mitigate such occurrences a variety of choices can be made. In order to address the amount of chloroform, a less toxic solvent could be used. However, thus far, research into the application of other solvents in the overall process of lutein and fame extraction from *C. vulgaris* is not as conclusive. In the case of mitigating methanol releases, a series of firefighting measures as well as the reduction of possible sources of ignition would be highly effective in allowing proper evacuation.

6.1.2 Chemical Compatibility

In investigating the chemical compatibility of various mixtures, a program named CRW4 was used to generate a chemical compatibility chart of common chemicals used in the process of this report.

Y : Compatible
N : Incompatible
C : Caution
SR : Self-Reactive
*: Changed by user

NFPA Health	NFPA Flammability	NFPA Instability	NFPA Special	Total Mixture Compatibility Chart	CHLOROFORM	ETHANOL	METHANOL	N-HEXANE	POTASSIUM HYDROXIDE, SOLUTION	SODIUM HYDROXIDE SOLUTION	SULFURIC ACID	WATER
2	0	0		CHLOROFORM								
2	3	0		ETHANOL	Y							
1	3	0		METHANOL	Y	Y						
	3	0		N-HEXANE	Y	Y	Y					
3	0	1		POTASSIUM HYDROXIDE, SOLUTION	N	N	N	Y				
3	0	1		SODIUM HYDROXIDE SOLUTION	N	N	N	Y	C			
3	0	2	llo	SULFURIC ACID	N	N	N	N	N	N		
				WATER	C	Y	Y	Y	C	C	C	

Figure 6.1-03: Chemical compatibility chart of common chemicals throughout process

Although most of the mixtures detailed here marked “N” are not present in the process, several occur in small quantities or the component chemicals are situated near enough to each other to pose a risk. A table below details the components in the mixture, the effects of such a mixture, and its presence in the process.

Table 6.1-02
Unintended Reaction Matrix

Component Mixture	Hazards	Location in Process
Chloroform + KOH	- Corrosive - Flammable - Pressurization - Toxic	- C15 & C17 contain large amounts - CMW & HEW extractions contain traces
Chloroform + NaOH	- Corrosive - Flammable - Pressurization - Toxic	- None
Chloroform + H_2SO_4	- Corrosive - Explosive - Pressurization - Toxic	- Trace in C3
Ethanol + KOH	- Flammable - Pressurization - Exothermic	- None
Ethanol + NaOH	- Flammable - Pressurization - Exothermic	- None
Ethanol + H_2SO_4	- Explosive - Flammable - Pressurization - Exothermic - Toxic	- C3
Methanol + KOH	- Flammable - Pressurization - Exothermic	- C13, C15, C17, & C19
Methanol + NaOH	- Flammable - Pressurization - Exothermic	- None
Methanol + H_2SO_4	- Explosive - Flammable - Pressurization - Exothermic - Toxic	- C6
n-Hexane + H_2SO_4	- Pressurization - Exothermic - Toxic	- None
KOH + H_2SO_4	- Corrosive - Pressurization - Exothermic - Explosive - Toxic	- None
NaOH + H_2SO_4	- Corrosive - Pressurization - Exothermic - Explosive - Toxic	- None

6.2 Societal Considerations

The development of this production facility in Duplin County, North Carolina, aimed at producing biodiesel and lutein presents both benefits and challenges to society.

Smithfield Hog Production is located in Duplin County, where hogs outnumber people by 30 to 1. This overabundance of hogs is causing the region to experience significant issues with hog waste management. This includes foul odors in the air and environmental pollution that disproportionately impacts Black and Brown, Latino, Indigenous, and low-income communities (Baars, 2024). The introduction of algae raceways, utilizing hog waste as nutrients for algae cultivation, offers a solution to mitigate the effects of hog production on the local environment and community health. This can potentially reduce water pollution and contribute to more sustainable waste management practices. It is important to ensure that the benefits of this operation are equitably distributed and that negative consequences are reduced to avoid unequally impacting marginalized communities. However, while using hog waste may assist in reducing smells in the air from hog production, the process of algae cultivation may still generate odors.

The creation of this plant additionally has the potential to create employment opportunities in the local communities. This includes jobs in fields such as management and administration, engineering, maintenance, production, quality control, environmental health and safety, logistics and supply chain, sales and marketing, and information technology. By employing individuals with diverse skill sets and expertise, this plant can foster career advancement, skill development, and professional growth.

Biodiesel and lutein are products that are advantageous to society. Biodiesel production offers a renewable and environmentally friendly alternative to fossil fuels. Biodiesel derived

from algae generates lower emissions of greenhouse gasses and pollutants compared to fossil fuels, contributing to cleaner air and decreased environmental degradation. This can help mitigate climate change and promote environmental sustainability while increasing national energy security and independence. The production of lutein from algae offers a wide variety of health benefits. It helps to improve eye health and protect against age-related vision loss and ocular diseases such as macular degeneration (Alves-Rodrigues & Shao, 2004). Overall, biodiesel and lutein help to address global health and environmental problems.

However, this plant necessitates a large quantity of land. 4,321 raceways are required for algae cultivation. This occupies 214 acres of land, which is equivalent to the area coverage of 162 football fields. Further space is needed for the extensive quantity of processing operations to convert the algae into biodiesel and lutein. Concerns may arise surrounding the allocation of land resources, particularly in areas where land availability is limited or where competing land uses, such as agriculture or conservation, are prevalent. The utilization of a significant amount of land for industrial purposes also may alter the landscape and aesthetics of the region. It would be important to engage with the local community to facilitate collaborative design of the plant and transparent communication, taking their concerns and preferences into account.

Furthermore, the operation of this plant involves large water usage. The largest consumption of water occurs in the raceways, where 83,300,000 kg/day of water are needed to create the optimal conditions for algae growth. Additionally, various other processing parts of the plant also require significant water input. This large water usage can impose demands on local water resources. This may impact local communities, agriculture, and ecosystems that rely on the same water sources.

6.3 Environmental Considerations

The presence of a variety of chemical hazards not only endangers lives of workers and communities in the vicinity of the manufacturing plant, but also puts the local fauna and environment at risk. Furthemore, the plant does not currently recycle a majority of the solvents, continuously creating an excess of hazardous waste and increasing the risk to the community. The risks posed by each of the different chemicals introduced is explored below:

1. Chloroform:

According to both government advice and safety data sheets provided by Sigma-Aldrich, Chloroform poses a risk to the environment primarily through water contamination. Given this, no chloroform should be allowed to enter drains or seep into the ground (Sigma-Aldrich, 2024a). The latter poses a significant risk given the ability for chloroform to remain in ground water or other dark and cold conditions due to the absence of light and heat. Should fish or other aquatic life come in contact, risk of acute and chronic toxic reactions are to be expected (Australian Government DCCEEW, 2023b). In order to prevent the release of chloroform into the environment, proper waste treatment or disposal of any waste streams containing even trace amounts of chloroform must be performed.

2. Ethanol:

Although toxic to aquatic organisms, it is not believed to persist in these environments. Additionally, contamination of groundwater as a result of ethanol does not seem to pose a danger (Fisher Scientific Company, 2022).

3. Glycerol:

A common byproduct of biodiesel refining, glycerol must be safely contained due to its possibility of soil contamination (Chilakamarry, 2021). As with most other chemicals in this process, draining them into water treatment systems is not advised (Sigma-Aldrich, 2024d).

4. Hexane:

Proven to be rather toxic to aquatic species, hexane is recommended to be kept away from drains (Mikkelsen et al., 2014). Additionally, hexane runs the risk of explosion in the wilderness potentially endangering animal life (Sigma-Aldrich, 2024b).

5. Lutein:

No known effects of lutein are known upon environmental release. However, caution is still advised against draining any lutein (Fisher Scientific Company, 2021).

6. Methanol:

The environmental impacts of methanol are primarily long term for wildlife and fauna. These primarily present themselves in reduced birth rates and birth defects in non aquatic life (Australian Government DCCEEW, 2023a; Fisher Scientific Company, 2015). Given this, any waste streams containing methanol must be treated or properly disposed of as hazardous waste to ensure that no methanol enters the sewer, the groundwater, or any other surface bodies of water.

7. Potassium Hydroxide:

Caution is advised in flushing potassium hydroxide down drains or into municipal/sanitary water systems (Fisher Scientific Company, 2023). Ground water is also

particularly prone to contamination thus care must be taken when disposing of streams containing potassium hydroxide.

8. Sodium Hydroxide:

Being readily degradable into non toxic products, sodium hydroxide poses a far smaller risk than most other chemicals used in the process (*Sodium Hydroxide Safety Data Sheet,* 2014). Although advised against draining, the water treatment plants in Duplin County would be able to process any water that was contaminated by this chemical.

9. Sulfuric Acid

The primary environmental threat posed by sulfuric acid at the concentrations used for our process (96% by weight) is primarily corrosivity towards fauna as well as respiratory complications in gaseous form (Amdur, 1989). As a result, safety data sheets advise against draining sulfuric acid and introducing it into the water sewage system (Sigma-Aldrich*,* 2024c).

7. Conclusions and Recommendations

The production of biodiesel and lutein from algae has significant potential as a sustainable solution to meet the growing energy and nutritional demands of our society. However, due to the current cost of production we cannot recommend that this plant be built.

To enhance the economic feasibility of producing biodiesel and lutein from algae, several areas of the project can be optimized. In terms of algae cultivation, exploring alternative growth systems that require less land or implementing strategies to maximize land use efficiency could help minimize costs and environmental footprint. Advancements in research and development, particularly in the field of nanotechnology, may lead to more cost-effective flocculation methods using nanomagnetite particles or other chemicals for DAF. As research progresses and these technologies become more accessible, the cost of flocculation could be significantly reduced and yield may improve. Additionally, finding more efficient ways to lyse, dewater, and dry the algae cells is essential. It is necessary for the cells to retain some water content for optimal yield in the bead mill process, meaning the dryers are required to dry the solution from 6% algae by weight to 90% algae by weight. As a result, the dryers constitute the highest capital cost of the project. Exploring other strategies to lyse and dry the algae may reduce the quantity of dryers and hot air needed, consequently decreasing capital and operating costs. In regards to chemicals used, both hexane and chloroform's uses could be optimized. Hexane contributes significantly to operational costs as none of it is reused necessitating a recycling method if operational costs are to be minimized. As waste management is a major source of operational costs and poses an environmental threat, process optimization including recycling solvents to ensure minimum quantities of hazardous chemicals onsite would be essential. Minimizing both economic and environmental risk would necessitate reducing the total amount of each solvent. Furthermore, it

is recommended to avoid using chloroform throughout the process due to its negative environmental and health impacts, which necessitate strict and expensive separation and waste disposal processes.

Overall, although this project offers positive aspects such as sustainable energy production, health benefits, job creation, and hog waste management, challenges in economic viability and land use must be addressed. Although the price of lutein and biodiesel are on an upwards trend, additional research, technological advancement, and refinement of the processes explored in this report are needed to overcome these hurdles and ensure long term success of the project.

8. Acknowledgements

We would like to thank Professor Eric Anderson for his invaluable help throughout the course of this project.

References

AFDC (2023). Alternative Fuels Data Center. ASTM Biodiesel Specifications. https://afdc.energy.gov/fuels/biodiesel_specifications.html

Agtec 45mil RPP Pond and Chemical Containment Geomembrane Liner (Custom Size). (2024). Retrieved April 4, 2024, from https://www.agriculturesolutions.com/agtec-45mil-rpp-pond-and-chemical-containment-geomembrane-liner-custom-size?gad_source=1&gclid=CjwKCAjwkuqvBhAQEiwA65XxQAlgPpUL8cMOmwol5wuB9lozsLMDVpg0tQcPrVuZATdeomYFGsl5_RoCbykQAvD_BwE

Alerts, I. (2019a, March). *Methanol prices: Current and forecast*. Intratec.us. https://www.intratec.us/chemical-markets/methanol-price

Alerts, I. (2019b, March). *Potassium hydroxide prices: Historical and current*. Intratec.us. https://www.intratec.us/chemical-markets/potassium-hydroxide-price

Alerts, I. (2019c, March). *Sulfuric acid prices: Historical and current*. Intratec.us. https://www.intratec.us/chemical-markets/sulfuric-acid-price

Alerts, I. (2019d, April). *Chloroform prices: Historical and current*. Intratec.us. https://www.intratec.us/chemical-markets/chloroform-price

Alerts, I. (2019e, April). *Ethanol price: Current and forecast*. Intratec.us. https://www.intratec.us/products/energy-price-references/commodity/ethanol-price

Alfa Laval Inc. (n.d.). *Separating oil from Olives - Alfa Laval.* Alfa Laval. https://www.alfalaval.com/globalassets/documents/products/separation/centrifugal-separators/decanters/pft00316en.pdf

Alves-Rodrigues, A., & Shao, A. (2004, April). The science behind lutein. *Toxicology Letters 150,* 57-83. https://doi.org/10.1016/j.toxlet.2003.10.031

Amdur M. O. (1989). Health effects of air pollutants: sulfuric acid, the old and the new. Environmental health perspectives, 81, 109–122. https://doi.org/10.1289/ehp.8981109

Andersen, D. (2018, July 19). The Manure Scoop: Manure Pumping – Viscosity, Flow Estimation, and going Beyond Hazen-Williams. *The Manure Scoop*. https://themanurescoop.blogspot.com/2018/07/manure-pumping-viscosity-flow.html

Araujo, G. S., Matos, L. J. B. L., Fernandes, J. O., Cartaxo, S. J. M., Gonçalves, L. R. B., Fernandes, F. A. N., & Farias, W. R. L. (2013). Extraction of lipids from microalgae by ultrasound application: Prospection of the optimal extraction method. *Ultrasonics Sonochemistry*, 20(1), 95–98. https://doi.org/10.1016/j.ultsonch.2012.07.027

Australian Government DCCEEW. (2023a, June 21). Department of Climate Change, Energy, \ the Environment and Water. *Chloroform (trichloromethane)*. https://www.dcceew.gov.au/environment/protection/npi/substances/fact-sheets/chloroform-trichloromethane#:~:text=Chloroform%20may%20be%20hazardous%20to,which%20the%20fish%20is%20taken.

Australian Government DCCEEW. (2023b, June 30). Department of Climate Change, Energy, the Environment and Water. *Methanol*. https://www.dcceew.gov.au/environment/protection/npi/substances/fact-sheets/methanol#:~:text=Drinking%20Water%20Guidelines.-,Description,affect%20their%20appearance%20or%20behaviour

Baars, S. (2024, March 8). *North Carolina's hog problem*. Southern Environmental Law Center. https://www.southernenvironment.org/news/the-sinister-hog-industry-of-eastern-north-carolina/

Banerjee, S., & Ramaswamy, S. (2019). Comparison of productivity and economic analysis of microalgae cultivation in open raceways and flat panel photobioreactor. *Bioresource Technology Reports*, 8, 100328. https://doi.org/10.1016/j.biteb.2019.100328

Black, A., Kwon, J., O'Quinn, T., & Yoshizaki, K. (2022). *Production of Biodiesel from Algae* [Unpublished bachelor's thesis]. University of Virginia.

Bligh, E. G., & Dyer, W. J. (1959). A rapid method of total lipid extraction and purification. *Canadian journal of biochemistry and physiology,* 37(8), 911–917. https://doi.org/10.1139/o59-099

Borowitzka, M.A. (2013). Energy from Microalgae: A Short History. *Algae for Biofuels and Energy,* 1-15. https://doi.org/10.1007/978-94-007-5479-9_1

Chastain, J. P., Camberato, J. J., Albrecht, J. E., & Adams, J. (n.d.). *Swine Manure Production and Nutrient Content*.

Chemical Plant Operator I Salary in North Carolina. (n.d.). Salary.Com. Retrieved March 22, 2024, from https://www.salary.com/research/salary/benchmark/chemical-plant-operator-i-salary/nc

Chilakamarry, C. R., Sakinah, A. M. M., Zularisam, A. W., & Pandey, A. (2021). Glycerol waste to value added products and its potential applications. Systems Microbiology and Biomanufacturing, 1(4), 378–396. https://doi.org/10.1007/s43393-021-00036-w

Chisti, Y. (2013). Raceways-based Production of Algal Crude Oil. *Green, 3*(3-4), 195-216. https://doi.org/10.1515/green-2013-0018

Christie, W.W. (1982). In: Lipid analysis (2nd Ed.) Pergamon Press:22
Eggers, L.F., Schwudke, D. (2016). Liquid Extraction: Folch. In: Wenk, M. (eds) *Encyclopedia of Lipidomics*. Springer, Dordrecht. https://doi.org/10.1007/978-94-007-7864-1_89-1

Danquah, M. K., Ang, L., Uduman, N., Moheimani, N., & Fordea, G. M. (2009). "Dewatering of microalgal culture for biodiesel production: Exploring polymer flocculation and tangential flow filtration," *J. Chem. Technol. Biotechnol*., *84*, 1078–1083. https://doi.org/10.1002/jctb.2137

El-Mashad, H. M., Zhang, R., & Avena-Bustillos, R. J. (2008). A two-step process for biodiesel production from salmon oil. *Biosystems Engineering*, 99(2), 220-227.

Electricity Local. (n.d.). *Warsaw Electricity Rates*. Retrieved April 5, 2024, from https://www.electricitylocal.com/states/north-carolina/warsaw/

EPA (2023, October 5). United States Environmental Protection Agency. Sources of Greenhouse Gas Emissions. https://www.epa.gov/ghgemissions/sources-greenhouse-gas-emissions

Fisher Science Education. (2015, August 1). *Methanol Safety Data Sheet*. Fisher Science Education.https://beta-static.fishersci.com/content/dam/fishersci/en_US/documents/programs/education/regulatory-documents/sds/chemicals/chemicals-m/S25426A.pdf

Fisher Science Education. (2014, December 14). *Sodium Hydroxide Safety Data Sheet*. Fischer Science Education.https://beta-static.fishersci.com/content/dam/fishersci/en_US/documents/programs/education/regulatory-documents/sds/chemicals/chemicals-s/S25881.pdf

Fisher Scientific Company. (2021, December 28). *Lutein Safety Data Sheet*. Thermo Fisher Scientific.https://www.fishersci.com/store/msds?partNumber=AC456160010&productDescription=LUTEIN%2C+90%25+1GR&vendorId=VN00032119&countryCode=US&language=en

Fisher Scientific Company. (2022, January 7). *Ethanol Safety Data Sheet*. Thermo Fisher Scientific.https://www.fishersci.com/msdsproxy?productName=A405P4&productDescription=ETHANOL+AHYD+HISTO+4L&catNo=A405P-4+&vendorId=VN00033897&storeId=10652

Fisher Scientific Company. (2023, October 13). *Potassium Hydroxide Safety Data Sheet*. Thermo Fisher Scientific.https://www.fishersci.com/msdsproxy?productName=P2503&productDescription=POT+HYDROXIDE+CERT+ACS+3KG&catNo=P2503&vendorId=VN00033897&storeId=10652

Flottweg SE. (n.d.). *Flottweg Tricanter®: The original 3 phase decanter centrifuge*. Flottweg. https://www.flottweg.com/product-lines/tricanterr/

Folch et al. (1951). *Journal of Biological Chemistry*, 191:833.

Fuad, N., Omar, R., Kamarudin, S., Harun, R., A., I., & W.A.K.G, W. A. (2021). Harvesting Marine Microalgae Nannochloropsis sp. Using Dissolved Air Flotation (DAF) Technique. *Sains Malaysiana*, *50*(1), 73–83. https://doi.org/10.17576/jsm-2021-5001-08

Geankoplis, C. J., Lepek, D., & Hersel, A. (2018). Transport Processes and Separation Process Principles. *Pearson*. https://learning.oreilly.com/library/view/transport-processes-and/9780134181592/xhtml/ch7.xhtml

Gong, M., Li, X., & Bassi, A. (2018). Investigation of simultaneous lutein and lipid extraction from wet microalgae using Nile Red as solvatochromic shift probe. *Journal of Applied Phycology*, *30*(3), 1617–1627. https://doi.org/10.1007/s10811-018-1405-6

Guo, M., Song, W., and Buchain, J. (2015, Feb.). Bioenergy and biofuels: History, status and perspective. *Renewable and Sustainable Energy Reviews 42,* 712-725. https://doi.org/10.1016/j.rser.2014.10.013

Hosseinizand, H., Lim, C. J., Webb, E., & Sokhansanj, S. (2017). Economic analysis of drying microalgae Chlorella in a conveyor belt dryer with recycled heat from a power plant. *Applied Thermal Engineering*, *124*, 525-532. https://doi.org/10.1016/j.applthermaleng.2017.06.047

HomeGuide. (2023, December 7). *2024 Cost To Build A Pond By Square Foot & Acre*. https://homeguide.com/costs/cost-to-build-a-pond

Hu, Q., Sommerfeld, M., Jarvis, E., Ghirardi, M., Posewitz, M., Seibert, M., & Darzins, A. (2008). Microalgal triacylglycerols as feedstocks for biofuel production: Perspectives and advances. *The Plant Journal*, 54(4), 621–639. https://doi.org/10.1111/j.1365-313X.2008.03492.x

Hu, W. (2014). Dry weight and cell density of individual algal and cyanobacterial cells for algae research and development [Thesis, University of Missouri--Columbia]. In *Submitted by University of Missouri—Columbia Graduate School.* https://mospace.umsystem.edu/xmlui/handle/10355/46477

Josephine, A., Kumar, T. S., Surendran, B., Rajakumar, S., Kirubagaran, R., & Dharani, G. (2022). Evaluating the effect of various environmental factors on the growth of the marine microalgae, Chlorella vulgaris. *Frontiers in Marine Science*, *9*. https://doi.org/10.3389/fmars.2022.954622

Kail, B. W., Link, D., Morreale, B. Determination of Free Fatty Acids and Triglycerides by Gas Chromatography Using Selective Esterification Reactions, *Journal of Chromatographic Science*, Volume 50, Issue 10, November/December 2012, Pages 934–939,

"Kenansville Climate, Weather By Month, Average Temperature (North Carolina, United States)—Weather Spark". (n.d.). Retrieved May 7, 2024, from https://weatherspark.com/y/20803/Average-Weather-in-Kenansville-North-Carolina-United-States-Year-Round

Kim, G. M., & Kim, Y. K. (2022). Drying Techniques of Microalgal Biomass: A Review. *Applied Chemistry for Engineering*, *33*(2), 145–150. https://doi.org/10.14478/ACE.2022.1007

Kose, A., & Oncel, S. S. (2017). Algae as a promising resource for biofuel industry: Facts and challenges. *International Journal of Energy Research*, *41*(7), 924–951. https://doi.org/10.1002/er.3699

Kumar, K., Mishra, S. K., Shrivastav, A., Park, M. S., & Yang, J. W. (2015). Recent trends in the mass cultivation of algae in raceway ponds. *Renewable and Sustainable Energy Reviews*, *51*, 875–885. https://doi.org/10.1016/j.rser.2015.06.033

Ladmin. (2019, March 22). *Economic Analysis of swine diet cost versus Manure Value*. Livestock and Poultry Environmental Learning Community.https://lpelc.org/economic-analysis-of-swine-diet-cost-versus-manure-value/#:~:text=With%20diet%20formulation%2C%20the%20value,of%20about%20%242.00%20per%20head

Landsearch. (n.d.). *Duplin County, NC Land for Sale*. Retrieved April 5, 2024, from https://www.landsearch.com/properties/duplin-county-nc

Leite, L. de S., Hoffmann, M. T., & Daniel, L. A. (2019). Coagulation and dissolved air flotation as a harvesting method for microalgae cultivated in wastewater. *Journal of Water Process Engineering*, *32*, 100947. https://doi.org/10.1016/j.jwpe.2019.100947

Manufacturers. (2023, January 30). *What is the price of n-hexane in January 2023?*. Junyuan Petroleum Group. https://junyuanpetroleumgroup.com/products/what-is-the-price-of-n-hexane-in-january-2023/

MBUX. (n.d.). Retrieved March 1, 2024, from https://www.alfalaval.us/products/separation/centrifugal-separators/separators/mbux/

Meher, L. charan, Sagar, D. V., & Naik, S. (2006). Renewable and sustainable. *Energy Rev*, 10.

Mercer, P. & Armenta, R.E. (2011). Developments in oil extraction from microalgae. Eur. J. *Lipid Sci. Technol*., 113: 539-547. https://doi-org.proxy1.library.virginia.edu/10.1002/ejlt.201000455

Miguel, F., Martín, A., Mattea, F., & Cocero, M. J. (2008). Precipitation of lutein and co-precipitation of lutein and poly-lactic acid with the supercritical anti-solvent process. *Chemical Engineering and Processing: Process Intensification*, 47(9), 1594–1602.

https://doi.org/10.1016/j.cep.2007.07.008

Mike. (2023, October 22). *Sodium hydroxide price index*. BusinessanalytiQ. https://businessanalytiq.com/procurementanalytics/index/sodium-hydroxide-price-index/

Mikkelsen, S. H., Warming, M., Syska, J., & Voskian, A. (2014). (rep.). *Survey of n-hexane* (pp.36–39). Copenhagen: The Danish Environmental Protection Agency.

Moradi-kheibari, N., Ahmadzadeh, H. & Hosseini, M. Use of solvent mixtures for total lipid extraction of Chlorella vulgaris and gas chromatography FAME analysis. *Bioprocess Biosyst Eng* 40, 1363–1373 (2017). https://doi.org/10.1007/s00449-017-1794-y

Narala, R. R., Garg, S., Sharma, K. K., Thomas-Hall, S. R., Deme, M., Li, Y., & Schenk, P. M. (2016). Comparison of Microalgae Cultivation in Photobioreactor, Open Raceway Pond, and a Two-Stage Hybrid System. *Frontiers in Energy Research*, *4*. https://doi.org/10.3389/fenrg.2016.00029

Niaghi, M., Mahdavi, M. A., & Gheshlaghi, R. (2015). Optimization of dissolved air flotation technique in harvesting microalgae from treated wastewater without flocculants addition. *Journal of Renewable and Sustainable Energy*, *7*(1), 013130. https://doi.org/10.1063/1.4909541

NC DEQ. (2023, July 1). North Carolina Department of Environmental Quality *Hazardous Waste Fees*. https://www.deq.nc.gov/about/divisions/waste-management/hazardous-waste-section/fees-and-records-management/hazardous-waste-fees

Ötleş, S. & Pire, R. Fatty Acid Composition of Chlorella and Spirulina Microalgae Species, *Journal of AOAC INTERNATIONAL*, Volume 84, Issue 6, 1 November 2001, Pages 1708–1714,

Pandey, R., & Premalatha, M. (2017). Design and analysis of flow velocity distribution inside a raceway pond using computational fluid dynamics. *Bioprocess and Biosystems Engineering*, *40*(3), 439–450. https://doi.org/10.1007/s00449-016-1712-8

Patel, A. K., Kumar, P., Chen, C.-W., Tambat, V. S., Nguyen, T.-B., Hou, C.-Y., Chang, J.-S., Dong, C.-D., & Singhania, R. R. (2022). Nano magnetite assisted flocculation for efficient harvesting of lutein and lipid producing microalgae biomass. *Bioresource Technology*, *363*, 128009. https://doi.org/10.1016/j.biortech.2022.128009

Peters, M. S., & Timmerhaus, K. D. (1991). *Plant design and economics for chemical engineers* (4th ed.). McGraw-Hill.

Peters, M. S., Timmerhaus, K. D., & West, R. E. (2003). *Plant design and economics for chemical engineers* (5th ed). McGraw-Hill.

Pharmacompass. (n.d.). *Lutein*. Retrieved April 5, 2024, from https://www.pharmacompass.com/active-pharmaceutical-ingredients/lutein

Portland Kettle Works. (n.d.). *Stainless Steel Chemical Mixing and Storage Tanks*. https://www.portlandkettleworks.com/chemical-mixing-and-storage-tanks/

Postma, P.R., Miron T.L., Oliveri, G., Barbosa, M.J., Wijffels, R.H., & Eppink, M.H.M. (2015). Mild disintegration of the green microalgae *Chlorella vulgaris* using bead milling. *Bioresource Technology, 184,* 297-304. https://doi.org/10.1016/j.biortech.2014.09.033

Postma, P.R., Suarez-Garcia, E., Safi, C., Yonathan, K., Oliveri, G., Barbosa, M.J., Wijffels, R.H., & Eppink, M.H.M. (2017). Energy efficient bead milling of microalgae: Effect of bead size on disintegration and release of proteins and carbohydrates. *Bioresource Technology, 224,* 670-679. https://doi.org/10.1016/j.biortech.2016.11.071

Prommuak, C., Pavasant, P., Quitain, A. T., Goto, M., & Shotipruk, A. (2013). Simultaneous Production of Biodiesel and Free Lutein from Chlorella vulgaris. *Chemical Engineering & Technology, 36(5)*, 733–739. https://doi.org/10.1002/ceat.201200668

Rahman, M. A., Aziz, M. A., Al-Khulaidi, R. A., Sakib, N., & Islam, M. (2017). Biodiesel production from microalgae Spirulina maxima by two step process: Optimization of process variable. *Journal of Radiation Research and Applied Sciences*, 10(2), 140-147.

Sakarika, M., & Kornaros, M. (2017). Kinetics of growth and lipids accumulation in Chlorella vulgaris during batch heterotrophic cultivation: Effect of different nutrient limitation strategies. *Bioresource technology*, *243*, 356–365. https://doi.org/10.1016/j.biortech.2017.06.110

Savvidou, M. G., Dardavila, M. M., Georgiopoulou, I., Louli, V., Stamatis, H., Kekos, D., & Voutsas, E. (2021). Optimization of Microalga *Chlorella vulgaris* Magnetic Harvesting. *Nanomaterials*, *11*(6), Article 6. https://doi.org/10.3390/nano11061614

SBPTA (n.d.). Small Business Property Tax Advisors. *Duplin County Property Tax Rates in 2023.* https://sbpta.com/duplin-county-property-tax-rates-in-2023/#:~:text=Duplin%20County%20has%20a%20tax,per%20%24100%20of%20assessed%20value.

Shi, X.-M., Chen, F., Yuan, J.-P., & Chen, H. (1997). Heterotrophic production of lutein by selected Chlorella strains. *Journal of Applied Phycology*, 9(5), 445–450. https://doi.org/10.1023/A:1007938215655

Sigma-Aldrich. (2024a, February 3). *Chloroform Safety Data Sheet*. Sigma Aldrich. https://www.sigmaaldrich.com/US/en/search

Sigma-Aldrich. (2024b, March 15). *Hexane Safety Data Sheet*. Sigma Aldrich. https://www.sigmaaldrich.com/US/en/sds/sial/296090?userType=undefined

Sigma-Aldrich. (2024c, March 7). *Sulfuric Acid Safety Data Sheet*. Sigma Aldrich. https://www.sigmaaldrich.com/US/en/sds/aldrich/339741

Sigma-Aldrich. (2024d, March 23). *Glycerol Safety Data Sheet*. Sigma Aldrich. https://www.sigmaaldrich.com/US/pt/sds/sigma/g2025

Smithfield Foods. (n.d.). Retrieved April 6, 2024, from https://www.smithfieldfoods.com/

Solubility of Air in Water. (n.d.). Retrieved February 3, 2024, from https://www.engineeringtoolbox.com/air-solubility-water-d_639.html

Statista. (2024). *Retail prices for B20 fuel, B100 fuel and regular diesel in the United States on the first of each month from January 2016 to January 2024*. Retrieved April 5, 2024, from https://www.statista.com/statistics/1200903/us-b20-retail-fuel-price/

Suarez-Garcia, E., Lo, C., Eppink, M.H.M., Wijffels, R.H., & van den Berg, C. (2019). Understanding mild cell disintegration of microalgae in bead mills for the release of biomolecules. *Chemical Engineering Science, 203,* 380-390. https://doi.org/10.1016/j.ces.2019.04.008

Sukenik, A., Bilanovic, B., & Shelef, G. (1988) Flocculation of microalgae in brackish and sea waters. *Biomass, 15*, 187–199. https://doi.org/10.1016/0144-4565(88)90084-4

Sündermann, A., Eggers, L.F., Schwudke, D. (2016). Liquid Extraction: Bligh and Dyer. In: Wenk, M. (eds) *Encyclopedia of Lipidomics*. Springer, Dordrecht. https://doi.org/10.1007/978-94-007-7864-1_88-1

Synder Filtration. (n.d.) *V0.1 (PVDF 0.1µm) Industrial MF Membrane*. Retrieved April 3, 2024, from https://synderfiltration.com/2014/wp-content/uploads/2019/01/V0.1-PVDF-0.1um-Industrial-Specsheet.pdf

Taghizadeh, S. M., Berenjian, A., Chew, K. W., Show, P. L., Mohd Zaid, H. F., Ramezani, H., Ghasemi, Y., Raee, M. J., Ebrahiminezhad, A., (2020). Impact of magnetic immobilization on the cell physiology of green unicellular algae Chlorella vulgaris. *Bioengineered, 11*, 141–153.

Turton, R., Shaeiwitz, J. A., Bhattacharyya, D., & Whiting, W. B. (2018). *Analysis, Synthesis, and Design of Chemical Processes* (5th ed.). O'Reilly.

Uduman, N., Qi, Y., Danquah, M. K., Forde, G. M., & Hoadley, A. (2010). Dewatering of

microalgal cultures: A major bottleneck to algae-based fuels. *Journal of Renewable and Sustainable Energy*, *2*(1), 012701. https://doi.org/10.1063/1.3294480

Vechpanich, J., & Shotipruk, A. (2010). Recovery of Free Lutein From *Tagetes erecta*: Determination of Suitable Saponification and Crystallization Conditions. *Separation Science and Technology*, *46*(2), 265–271. https://doi.org/10.1080/01496395.2010.506904

Vicente, G., Martınez, M., & Aracil, J. (2004). Integrated biodiesel production: a comparison of different homogeneous catalysts systems. *Bioresource technology*, *92(3)*, 297-305.

Villagracia, A. R. C., Mayol, A. P., & Ubando, A. T. (2016). Microwave drying characteristics of microalgae (Chlorella vulgaris) for biofuel production. *Clean Techn Environ Policy,* 18, 2441–2451. https://doi.org/10.1007/s10098-016-1169-0

WAB Group. (n.d.). *High-performance Agitator Bead Mill DYNO-MILL ECM-AP*. Retrieved March 13, 2024, from https://www.wab-group.com/en/products/dyno-mill-ecm-ap/

Waterwheel Factory. (2024). *Pricing*. Retrieved April 4, 2024, from https://waterwheelfactory.com/price.html

Yu, W., Liu, R., & Yang, W. (2020). Parameter Calibration of Pig Manure with Discrete Element Method Based on JKR Contact Model. *AgriEngineering*, *2*(3), Article 3. https://doi.org/10.3390/agriengineering2030025